Environmental
Studies
Revolving
Funds

022

Enhancement of the Radar Detectability of Icebergs

Canada

January 1986

The Environmental Studies Revolving Funds are financed from special levies on the oil and gas industry and administered by the Canada Oil and Gas Lands Administration for the Minister of Energy, Mines and Resources, and by the Northern Affairs Program for the Minister of Indian Affairs and Northern Development.

Environmental Studies Revolving Funds
Report Series No. 022

January 1986

ENHANCEMENT OF THE RADAR DETECTABILITY OF ICEBERGS

Joseph P. Ryan
Viatec Resource Systems Inc.
P. O. Box 5414
St. John's, Newfoundland
A1C 5W2

The correct citation for this report is:

Ryan, Joseph P. 1985. Enhancement of the Radar Detectability of Icebergs. Environmental Studies Revolving Funds Report No. 022. Ottawa. 93 pp.

Published under the auspicies
of the Environmental Studies
Revolving Funds
ISBN 0-920783-21-X

TABLE OF CONTENTS

LIST OF TABLES

LIST OF FIGURES

ABBREVIATIONS

The following acronyms are used in the text:

CODAR	Coastal ocean dynamics applications radar
HF	High frequency band (3 - 30 MHz)
IIP	International Ice Patrol
LORAN	Long range aid to navigation
LP	Long pulse
MP	Medium pulse
SWH	Significant wave height

PARAMETERS

The following terms are used in the text and in equations:

A	Iceberg area projected towards the radar
F	Propagation factor
G	Antenna gain (dB)
h_a	Antenna height
L	Radar losses
P_d	Probability of detection
P_{fa}	Probability of false alarm
P_r	Power received (Watts)
P_t	Peak transmitter power (Watts)
R	Range to iceberg (m)
τ	Pulse length (microsec.)
σ	Radar cross-section (m^2)
θ	Beamwidth (deg.)
λ	Radar wave length (m)
σ^o	Back-scatter coefficient (m^2/m^2)

ACKNOWLEDGEMENTS

The author would like to acknowledge the assistance provided by Derek Strong of COGLA and Jacques Benoit of Mobil Oil Canada Ltd. Discussions on radar cross-section estimation with Byron Dawe of NORDCO Ltd. and Dr. John Walsh at Memorial University of Newfoundland are also appreciated. The scientific adviser for this study, Dave Pearson of Petro-Canada, has provided important input to this study on scientific and operational concerns.

SUMMARY

A study has been undertaken to investigate the use of enhancement techniques to increase the radar detectability of icebergs. These techniques will permit more efficient use of iceberg management tools such as support vessels and aircraft. There are essentially two strategies to achieve enhancement available; namely, passive and active. Passive techniques refer to those which increase the icebergs effective echoing area or radar cross-section and include the deployment of reflective material on the iceberg surface as well as a number of reflector configurations based on balloon and kite systems. Active techniques include the use of radar transponders, radio direction finding equipment, radio navigation equipment and satellite tracking systems.

The study has demonstrated that passive techniques may be used to increase the probability of detection of icebergs as well as increasing the detection or tracking range. The passive methods considered offer a very inexpensive way of improving iceberg tracking capability. These enhancement techniques will only be effective within the radar horizon (typically 35 km for a derrick top radar).

Active methods may be employed for ranges beyond the radar horizon. These techniques can provide from 50 to 500 km tracking ranges depending on the system used.

Recommendations from this study include field trials for the identified passive enhancement techniques and an evaluation of the operational requirements for both passive and active methods.

RÉSUMÉ

Une étude a été entreprise pour déterminer l'utilisation des techniques visant à améliorer la détection des icebergs par radar. Ces techniques permettront une utilisation plus efficace des outils de contrôle des icebergs comme par exemple les bateaux ravitailleurs et les avions. Il y a seulement deux stratégies possibles pour obtenir de meilleurs résultats: la méthode passive et la méthode active. On appelle techniques passives celles qui augmentent la portion de l'iceberg capable de renvoyer un écho ou balayage du radar et qui comprennent l'utilisation de matériel réfractaire basé sur un système de ballons et de cerfs-volants qui sont déployés à la surface de l'iceberg. Les techniques actives sont celles qui utilisent des transpondeurs, de l'equipement pour trouver la direction des ondes radio, de l'equipement de radio-navigation et des systèmes de repérage par satellite.

L'étude a démontré que les techniques passives peuvent etre utilisées afin d'augmenter la probabilité de détection des icebergs ainsi que la portée de détection ou repérage. Les méthodes passives sont considérées comme un moyen peu coûteux d'améliorer la capabilité de repérage des icebergs. Ces techniques d'amélioration ne peuvent être efficaces que dans les limites de l'horizon du radar (typiquement 35 km pour un radar installé au sommet du derrick).

On peut employer les méthodes actives pour des distances au-delà de l'horizon du radar. Ces techniques peuvent permettre de repérer des icebergs à une distance variant de 50 à 500 km suivant le système utilisé.

Dans les recommendations qui découlent de cette étude, on inclut des essais sur place des techniques passives d'amélioration du repérage des icebergs ainsi qu'une évaluation des méthodes passives et actives.

1. INTRODUCTION

Previous studies and operational experience indicate that marine radar is a major tool for detecting and avoiding ice hazards in support of offshore oil exploration. The ability of radar to detect icebergs is highly dependent on iceberg characteristics as well as environmental conditions. Once an iceberg has been detected, it is tracked until it no longer poses a threat to ongoing activities.

The iceberg tracking range will be increased by enhancing the radar return from the iceberg. This enhanced tracking capability will aid offshore operations by providing continuous and reliable iceberg detection beyond existing capabilities.

The radar return from the iceberg may be directly increased by increasing the iceberg's radar cross-section or effective echoing area. The radar cross-section is highly dependent on its size, shape and reflective properties. It is not possible to increase an iceberg's physical size and altering its shape to provide a greater cross-section is not yet feasible, however, by introducing highly reflective foreign material on or near the iceberg, the radar cross-section may be increased significantly. The techniques which make use of an enhanced cross-section or false cross-section fall in the category of passive techniques. Active techniques may be used which utilize radar transponders that are interrogated by the tracking radar. These transponders may be of the conventional type (i.e. microwave) or the HF (High Frequency) type applicable for use with HF radars such as CODAR (Coastal Ocean Dynamics Application Radar).

While target enhancement schemes may be useful for near range tracking (i.e. within the radar horizon), for longer ranges alternate systems are required. Lower frequency radio beacon and radio navigation systems can provide tracking ranges in excess of 150 km while satellite trackings systems are virtually unlimited in their tracking range.

The following report details enhancement/tracking systems which could be utilized with icebergs. The systems are separated into three main categories based on iceberg size. The iceberg size will dictate to some extent the potential threat and, hence, the maximum tracking range of interest. The three categories are:

a) Growler/bergy bit size icebergs:

These icebergs, which are typically less than 5 m in height, are difficult to detect and track at all ranges, even in low sea states. Frequently, these targets are obscured by waves. The enhancement method should address detection in clutter as well as obscuration by waves.

b) Small/medium icebergs:

With heights from 5 to 45 m, these icebergs are typically detected at ranges less than the radar horizon. The typical horizon for radars mounted on the derrick top of a semi-submersible is about 36 km and for those on support vessels it is about 16 km. The enhancement method should extend the tracking range of these targets to the radar horizon and further.

c) Large/very large icebergs:

Icebergs having heights greater than 45 m are typically detected to the radar horizon under normal propagation conditions. The enhancement/tracking system should extend the tracking range of these hazards to well beyond the radar horizon.

Chapter 2 of the report contains a literature review of the subject, detailing some early work on iceberg tagging as well as ongoing research in the area. Chapter 3 provides a discussion of available radar models and examples of present iceberg detection capability for various iceberg sizes and environmental conditions. Chapter 4 presents the various enhancement/tagging techniques which could be used to enhance the radar detectability of icebergs. In Chapter 5 each method is analyzed from the point of view of increased tracking range for a high probability of detection and details the costs and benefits associated with the enhancement techniques, and Chapter 6 provides conclusions and recommendations.

2. LITERATURE REVIEW

Some of the earliest work concerning the tracking of individual icebergs was carried out by the International Ice Patrol (IIP) of the United States Coast Guard. Before 1960, the IIP assigned surface vessels to follow icebergs from the time of their leaving well-defined ice-infested areas until they melted (Lenczyk, 1965). During the 1960s it was found that during good weather conditions icebergs could be tracked reliably with aircraft, however, bad weather often necessitated the use of iceberg drift and deterioration models to help re-identify icebergs on subsequent flights. Researchers have tried to mark individual icebergs for identification in several ways.

Kollmeyer used a bow and arrow and test tubes filled with various dyes to mark a position on the face of the iceberg (Robe, 1978). A similar method for iceberg marking was used by a Memorial University team to mark icebergs from a ship employing a bow and dye-tipped arrow (Allen, 1971). Another dyeing method used was to drop dye in containers from a tracker plane. Over the years the IIP reports limited success with this technique with the dye being usually washed away in one to two days. More recently the Canadian Forces Maritime Command experimented with dye marking from an airplane (Grant, 1971). Grant reports on an experiment with different types of containers for carrying the dye, as well as dye characteristics such as durability and visibility.

In 1974, the United States Coast Guard Oceanographic Unit began a project to determine the best way to tag an iceberg for identification and relocation. In 1974 Hayes attempted to tag icebergs using a floating line (Robe, 1977). The 0.95 cm polypropylene line was provided with additional floatation, as well as radar reflectors and a Radio Direction Finder transmitter. Limited success was reported using this method. In stormy conditions two of three icebergs being tracked broke free from the tagging array. Under calm conditions several icebergs were successfully tracked for nine days. The major problem identified with this method was the tendency for small deteriorated icebergs to roll out of the loop.

Robe (1978) identifies three main problems to be solved in order to attach an instrument package or tagging/enhancement device. These are iceberg rolling, iceberg melting and iceberg calving. In 1975 the Coast Guard Research and Development Center attempted to tether an instrument package to an iceberg using a large steel

dart and trailing line. The method effectively solved the problem of rolling and melting, however, calving would still pose a problem. Tests with the tethering technique carried out in 1975 and 1977 have demonstrated the capabilities of this technique.

Harwood (1971) discusses the tracking problem as related to icebergs and indicates that the Defence Research Establishment in Ottawa had contracted Marconi Electronics Company to develop an instrument package capable of being deployed on or near an iceberg with the capabilities of transmitting iceberg (instrument) position information derived from LORAN or other navigation equipment.

The literature survey has not revealed past work concerning the use of active radar devices for iceberg tracking (i.e. the use of radar transponders), however, the Bedford Institute of Oceanography in Nova Scotia has very successfully used radar transponders to track meteorological buoys for 15 days at a time (Parsons, Personal Communication). While dyeing methods have been considered by previous researchers, no reports concerning the use of radar reflective paint or substance have been identified. Nor have there been any reports of attempts to embed reflective material into an iceberg. Another area applicable to this study is the field of Electronic Warfare (EW) and the use of techniques of generating false radar targets by the use of chaff and other means. A good review of the types of chaff and their reflective properties is contained in Butters (1982).

3. THEORETICAL EVALUATION OF EXISTING ICEBERG DETECTION

The accurate prediction of received radar signal strength from iceberg targets in open ocean is necessary for both assessing a radar's iceberg detection capability, as well as estimating the increased tracking range resulting from the use of an enhancement technique. This chapter concentrates on an evaluation of radar models presently in use and provides tabular output of probabilities of iceberg detection for a number of environmental conditions. This present detection capability is used for comparison purposes in later discussions on the effectiveness of different enhancement techniques.

3.1 RADAR MODELS

A radar model of received signal strength from an iceberg must take into account the characteristics of the iceberg, the propagation path between the iceberg and the radar, the prevailing environmental conditions and the radar parameters. In addition, in order to provide an estimate of the detectability of the iceberg, it is necessary to model the competing signals such as sea clutter, rain clutter and receiver noise. The signal to noise plus clutter ratio may be used with published curves to derive the probability of detection, or alternatively expressions for the probability of detection may be incorporated into a computer model.

A computer model developed and presently used by Viatec provides such an output. For any given set of radar parameters and environmental conditions for X-band (9-10 GHz) and S-band (3 GHz), the model produces probability of detection as a function of range. The propagation model is based on the work of Kerr (1951) as presented by Blake (1980) and takes into account the earth's curvature, the ocean roughness and the atmospheric refractive index.

The choice of models for sea clutter and iceberg radar cross-section are still, to some extent, open for discussion. The model for sea clutter used here is based on the published values of the average back-scatter coefficient of the ocean surface as a function of grazing angle presented in Nathanson (1969). Nathanson presents average data from a number of different experiments.

Fairly good agreement was obtained with the Nathanson data by Ryan et al. (1985a) in an oil rig based experiment. Comparison of this experimental data with the model of Sittrop (1977) showed the experimental data to be about 5 dB (decibel) below the Sittrop model at grazing angles greater than 0.9° (see Fig. 3-1).

Based on this experiment, and more recent field work conducted by Viatec in a ship based experiment, it is suggested that until a more comprehensive model (i.e. one that takes into account the present sea condition including both wave information as well as wind speed) is developed, that the Nathanson data can be taken as being representative as average data.

Several models for iceberg radar cross-section are presently in use. These models are based mainly on the empirical fitting of experimental data for the normalized cross-section, $\sigma°$, available for different grazing angles and frequencies, to expressions for $\sigma°$ as a function of angle.

Dawe (1985) presents a model for $\sigma°$ based on applying Budinger's (1960) description of an iceberg's surface as "an aggregate of concave and convex curved surfaces of diameter greater than 1.3 in. (X-band wave length)" to a rough surface scattering model given by Barrick (1970). The rough surface model essentially reduces to the standard Fresnel reflection coefficient at vertical incidence modified by the surface roughness. He assumes that the surface has a Gaussian surface height correlaton coefficient and that the iceberg's loss tangent is negligible. The model requires that one know the surface height correlation length and the root mean square height of the surface roughness. Dawe derives these quantities from experimental data of Gray et al. (1979) for a frequency of 13.3 GHz. Extrapolation of this result to 10 GHz provides an expression for $\sigma°$ at X-band. Arguing that on average the slope of randomly oriented facets on an iceberg face will be 45° for all icebergs except for tabular and blocky icebergs, Dawe gives values of $\sigma°$ of -11.0 dB for tabular and blocky icebergs and -18.5 dB for all other types of icebergs.

The back-scatter coefficient, $\sigma°$, is given here in decibels where $\sigma°_{dB} = 10 \log \sigma°$ (log is the logarithm to base 10), so that for the cases where $\sigma°$ is 0.1 and 10 in natural units (real world), $\sigma°_{dB}$ will be -10 dB and +10 dB respectively.

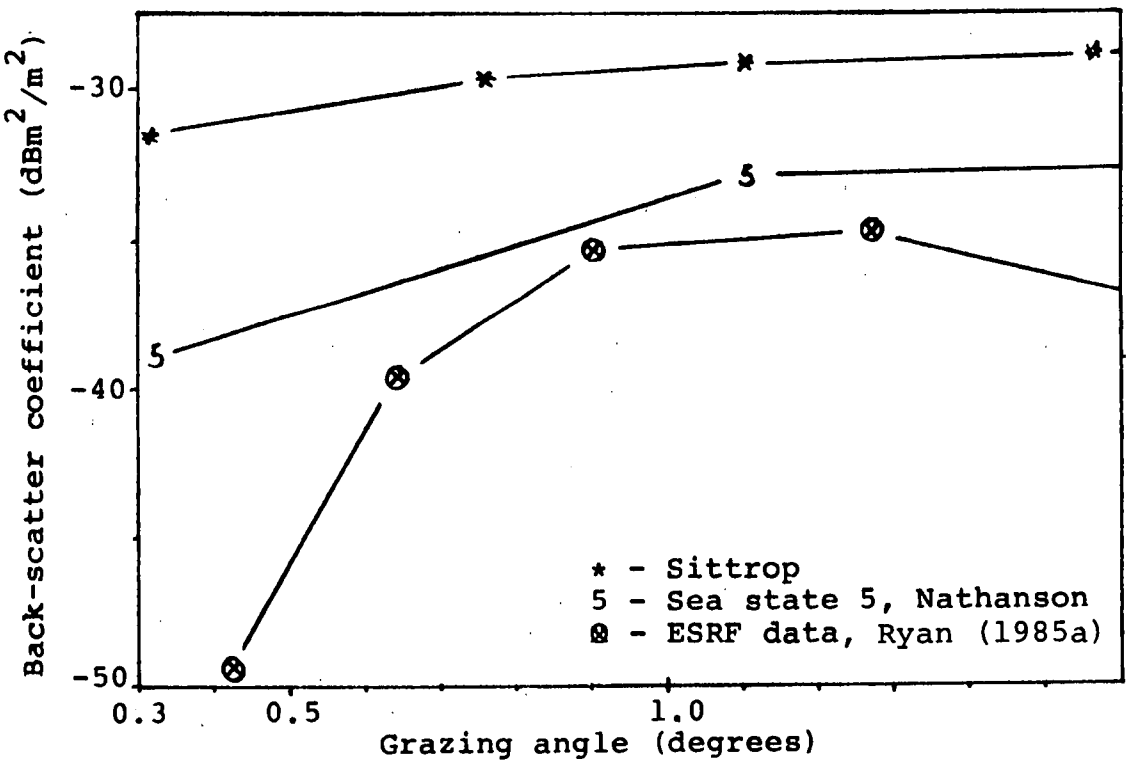

Fig. 3-1. Comparison of measured ocean back-scatter coefficients at X-band for a significant wave height of 2.6 m and a wind speed of 37 kts with tabulated values of Nathanson (1969), Sittrop (1977), and Ryan (1985a).

Another model presently in use was developed by Intera Technologies Ltd. for Mobil Oil and is also based on the derivation of σ° from experimental data. The radar cross-section is calculated by integrating the expression for σ° over the iceberg's area, A. Although the expression for σ° is proprietary, sets of curves were presented by Lowry et al. (1984) and an expression for the radar cross-section of an iceberg with projected cross-sectional area of A m^2 may be derived from these. The Intera model assumes a hemisphere shaped iceberg having a radius, r, giving an above water area of $(\pi r2)/2$.

Using this geometry the Intera model predicts a back-scatter coefficient of -19.0 dB for a wet iceberg and -11 dB for a dry iceberg. This range of values agrees remarkably well with the values presented by Dawe.

Another major work in this area was that of Budinger (1960). He reported on experimental data collected on the Grand Banks in 1959. The data consists of maximum range of detection for 152 different iceberg targets. From these observations he has derived empirically a normalized radar cross-section of -12.5 dB. Dawe (1985) states that this value is biased high due to a contribution of about 6 dB from the multipath propagation factor which Budinger neglects. The brief analysis in Appendix 1 indicates that the contribution to the signal strength due to integration over a target's height would be on average 6 dB and this is for a flat, perfectly smooth sea. For a spherical, rough sea the propagation factor will be less than 6 dB and is expected to contribute about a 3 to 4 dB increase in signal strength. As Budinger's data represents to some extent the average situation, an estimate of σ° from his data allowing for an average propagation factor of 4.5 dB would be -17.0 dB. As one can see from the discussion the two independent empirical derivations agree quite well and both are within 3 dB of the measured values of Budinger. The data collected by Ryan et al. (1985a) falls within the 5 dB range of the Budinger relationship and hence is also within acceptable range of the Dawe and Intera models. More recent ship-based field trials, Ryan et al. (1985b), indicate that the back-scatter coefficient for X-band is closer to the -11 dB value, while S-band is about 7 to 8 dB below this value at -18 dB. The relationship between σ° and the radar cross-section σ is defined as,

$$\sigma = \sigma^\circ A \qquad (3.1)$$

or

$$\sigma_{dB} = 10 \log \sigma^\circ + 10 \log A$$

where

A = area projected towards the radar in m^2
σ° = normalized radar cross-section

In modelling the return signal strength from an iceberg in open ocean, it becomes important to consider the propagation factor, F. For certain radar problems, such as the detection of high flying airplanes, F is usually taken to be unity, however, for height extensive (i.e. not point targets) targets at sea, the propagation factor must be included in the calculation. The received signal strength is given by:

$$P_r = \frac{P_t G^2 \lambda^2 F^4 \sigma}{(4\pi)^3 R^4 L} \qquad (3.2)$$

where

P_r = received power, watts
P_t = transmitter peak power, watts
G = antenna gain
λ = radar wave length
σ = radar cross-section of the iceberg = $\sigma^\circ A$
R = range to the iceberg
L = radar system losses
σ° = normalized radar cross-section
F = propagation factor
A = projected area of the iceberg facing radar

For targets having scatterers over its entire height, as is the case with icebergs, it is often difficult to separate the radar cross-section from the propagation factor as there is an effective integration of the signal strength over the iceberg's height. Table 3-1 presents a comparison of the quantity σF^4 for the three available models. These are calculated using Viatec's propagation model. (Note: The Intera model and the Budinger relationship assume F^4 is unity.) The range of values for the Dawe model is computed for a very rough sea (significant wave height of 7 m) a moderate sea (SWH = 2.5 m) and a smooth sea (SWH = 0.5 m).

It may be seen from this Table that using the back-scatter coefficients of Dawe or Intera with Viatec's propagation model yields results close to those for Budinger's relationship for a calm sea. For a rough sea, the propagation factor approaches unity (0.0 dB) which is the assumption of the Intera model.

In summary, the Dawe model for blocky and tabular icebergs and the Intera model for dry icebergs provide an optimistic radar cross-section while Dawe's model for other types of icebergs and Intera's wet iceberg model provide a pessimistic radar cross-section. This pessimistic cross-section when used with the Viatec propagation model should provide a good estimate on the lower bound of iceberg detection capability.

TABLE 3-1

Comparison of radar models for a 100 m^2 (projected area) iceberg having a 10 m height.

	Dawe			Intera (Wet Iceberg)	Budinger
$\sigma°$ (dB)	-18.5			-19.0	-12.5 to -18.5
σ (dB)	1.5			1.0	7.5
	SWH(m)				
	0.5	2.5	7.0		
F^4 (dB)	4.8	4.4	1.6		
σF^4 (dB)	6.3	5.9	3.1	1.0 dB	7.5 dB

Note: F^4 for the Dawe model is calculated with Viatec's propagation model at a range of 12 km.

3.2 PRESENT ICEBERG DETECTION CAPABILITY

In this section the Viatec radar model is utilized to produce tables of iceberg detection ranges as a function of iceberg size and environmental conditions. These detection ranges are calculated using average radar cross-sections for the iceberg, as well as clutter and therefore assumes that some scan-to-scan processing is used, whether it be in hardware or the use of a skilled operator. As a consequence the probability of detection is calculated in clutter limited cases by considering only single pulse detection, however, for noise limited detection the effect of pulse to pulse integration is included. The detection range is set by a probability of detection of 50% with a false alarm rate of 10^{-6} (i.e. one false alarm every 10^6 pulses). Appendix 2 contains a set of curves of probability of detection as a function of range, iceberg size and sea conditions. These curves are summarized in Tables 3-2 and 3-3 and the specifications of the radars are given in Table 3-4.

From these Tables, it is possible to get a good indication of the detection capability of a derrick (75 m) or ship (15 m) mounted dual radar (X and S Band) system. The derrick mounted systems will provide better long-range detection due to their longer horizon range. The lower radars will provide better performance in sea clutter limited situations with S-band providing detection to 8 km for a bergy bit (7 m x 15 m x 15 m) in sea state 5 (SWH = 2.5 m) utilizing medium pulse. Tables 3-2 and 3-3 indicate that in clutter limited situations there is often a zone of detection. For example the bergy bit mentioned above will be detected in the range from 11 to 17 km (6 to 9 naut mi) in sea state 5 from a derrick mounted radar. Closer than 11 km and the iceberg is lost in sea clutter. This is an example of how a low (15 m high) antenna can be used for near range detection and derrick mounted antennas used for long range detection. This was a well observed phenomena during a recent ESRF field experiment.

Although the Tables present the ranges for a probability of detection of 50%, this is on a single scan basis. For a trained operator, this is an acceptable detection level when the display is observed over a period of minutes. The curves in Appendix 2 may be used to find the detection ranges for any probability of detection.

This discussion of detection capability will serve as the basis for evaluating the increased detectability of the icebergs using the various enhancement and tagging techniques present in the next chapter.

TABLE 3-2

Detection capability of S-band radar
(Pd = 0.5, pfa = 10^{-6}).

			Range (km) LP/MP				
			Iceberg above water size H x L x W (m)				
SWH	Sea state	ha	2x5x5	4x10x10	7x15x15	25x60x60	45x110x110
		15	1/3	5/6	8/9	17/18	24/25
0.5	1	75	ND/7	12/13	17/18	32/33	40/41
2.5	5	15	ND/ND	ND/ND	ND/8	17/17	24/24
		75	ND/ND	ND/ND	ND/11-17	32/33	40/41
5.0	6	15	ND/ND	ND/ND	ND/6-7	17/17	24/25
		75	ND/ND	ND/ND	ND/ND	15-32/33	40/41

Notes: ND = probability of detection less than 50%
ha = antenna height (m)
SWH = significant wave height (m)
LP = radar long pulse = 1.0 μsec
MP = radar medium pulse = 0.25 μsec
Pd = probability of detection
pfa = probability of false alarm

TABLE 3-3

Detection capability of X-band radar
(Pd = 0.5, pfa = 10-6).

			Range (km) LP/MP				
			Iceberg size H x L x W (m)				
SWH	Sea state	ha	2x5x5	4x10x10	7x15x15	25x60x60	45x110x110
0.5	1	15	3/5	7/8	11/12	20/21	27/28
		75	ND/ND	ND/2-12	3-14/16	28/31	35/38
2.5	5	15	ND/ND	ND/ND	ND/5-10	20/21	27/28
		75	ND/ND	ND/ND	ND/ND	ND/31	35/38
5.0	6	15	ND/ND	ND/ND	ND/ND	12-20/21	27/28
		75	ND/ND	ND/ND	ND/ND	ND/ND	29-34/37

Notes: Same as for Table 3-2.

TABLE 3-4

Radar specifications

X-band	
Transmitter power:	25 kw
Antenna gain:	32 dB
Frequency	9410 MHz
Antenna beamwidth:	0.8 deg.
Minimum detectable signal:	-100 dBm
Losses:	4 dB
S-band	
Transmitter power:	30 kw
Antenna gain:	27 dB
Frequency:	3050 MHz
Antenna beamwidth:	2.0 deg.
Minimum detectable signal:	-100 dBm
Losses:	4 dB

4. ENHANCEMENT AND TAGGING TECHNIQUES

The tracking range for an iceberg may be increased by the use of passive enhancement techniques or active tagging methods. Passive techniques include radar cross-section enhancement by the modification of iceberg reflective properties or the use of reflectors situated on and off the iceberg. Active methods which are considered include the use of radar transponders, radio direction finding systems, satellite tracking systems and radio navigation systems. Passive and active techniques will be discussed in the following sections with reference to the size of iceberg for which the technique will be applicable and predicted improvements in iceberg radar cross-sections.

4.1 PASSIVE TECHNIQUES

The detectability of an iceberg may be increased in almost any situation by increasing its radar cross-section or effective echoing area. An iceberg's radar cross-section is dependent on its physical characteristics, such as size and shape, and on its electrical properties including conductivity and relative permittivity (dielectric constant). Typically the radar cross-section increases with iceberg size and icebergs with flat, vertical faces (i.e. blocky or tabular type) will exhibit higher cross-sections than those that are rounded or dome shaped. The reflectivity of the iceberg is dependent on the electrical properties of the ice and on the angle of incidence of the radar energy. As glacial ice contains no brine, its conductivity and permittivity are low in comparison to sea water and, as a result, sea water is about three times as reflective as iceberg ice. The simplest case of back-scatter from an iceberg is for an incidence angle of 90° (i.e. for a radar looking at a vertical face of a tabular or blocky iceberg) and at this incidence angle the reflection coefficient, Γ , may be approximated by the expression,

$$\Gamma = \frac{1-\sqrt{\varepsilon}}{1+\sqrt{\varepsilon}} = 0.28 \qquad (4.1)$$

where

ε = relative permittivity or dielectric constant

$\varepsilon \simeq 3.1$ Budinger (1960)

The back-scatter coefficient or normalized radar cross-section is given by,

$$\sigma^\circ = \Gamma^2 \qquad (4.2)$$
$$= 0.078 \text{ or } -11 \text{ dB}$$

which is the value used by Dawe (1985) for a tabular or blocky iceberg. If the iceberg has a projected area (i.e.: area projected towards the radar) of 100 m^2, then its radar cross-section will be 7.8 m^2 ($\sigma = \sigma^\circ A$). A highly conductive steel plate having the same area, will give a radar cross-section of about 123 million m^2 while a highly conductive sphere having the same projected area will give a radar cross-section of 100 m^2.

This discussion indicates that changes in the surface conductivity (i.e. electrical resistance) and shape of an iceberg will greatly influence its radar cross-section. Several methods have been considered which introduce conductive material onto the surface of the iceberg. They include the use of "chaff" material either secured to surface or embedded in the iceberg, as well as the use of highly reflective mesh. The other major passive enhancement technique consists of the use of radar reflectors situated on buoys, balloons or kites and tethered to the iceberg. The cross-section of the reflector will either enhance the iceberg's cross-section (i.e.: when both the iceberg and the reflector are in the same resolution cell) or provide a distinct echo larger than the iceberg's. These passive techniques will only be useful within the radar horizon and hence will be more applicable to smaller icebergs in the range from growlers to medium icebergs.

I) Resonant filaments:

Since the early stages of the Second World War, metallic strips have been used to confuse radar systems. Chaff, as it became known as, consists of thin metallic material cut in lengths approximately one-half of a radar wave length (one-half the X-band wave length is about 1.6 cm). This length will provide resonant scatter from each filament thereby maximizing the radar cross-section. Butters (1982) reports that a chaff filament with a random orientation will have a radar cross-section of:

$$\sigma = 0.172 \ \lambda^2 \qquad (4.3)$$

where

λ is the radar wave length (m)

In order to obtain a radar cross-section of 10 m2, about 57,000 of these filaments are required at X-band(λ = .032) and only 5800 at S-band (λ = 0.1). Typical chaff load density is on the order of 1 million filaments (or dipoles) per 100 g.

Chaff is designed to be released or fired into the air where it blooms into a cloud thereby providing a large volume of reflective material. A chaff cloud can last for 10 to 15 minutes, depending on the type of filament used and prevailing meteorological conditions (i.e.: wind, precipitation, etc.). It may be possible to use chaff in its available configuration (see Appendix 3) for short-term enhancement applications by distributing the chaff filaments over the iceberg. Longer enhancement periods may require a method of securing the filaments to the iceberg face.

Two alternatives to standard chaff have been investigated for enhancing the detectability of icebergs using chaff like dipoles. The first alternative, chaff ribbon, consists of chaff dipoles secured together in a plastic sleeve. This plastic sleeve could hold on the order of several thousand dipoles and be attached to the iceberg using a dart and line throwing gun. Several of these ribbons could be attached as illustrated in Fig. 4-1.

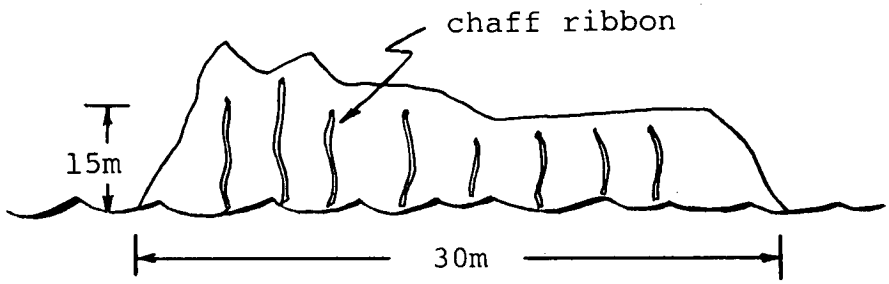

Fig. 4-1. The deployment of chaff ribbon on an iceberg.

For a 15 m high iceberg it is expected that about 10 m of effective ribbon length would be exposed. It is necessary for the dipoles to be separated by at least 2 radar wave lengths such that mutual coupling does not cause a deterioration of the dipole radar cross-section. Therefore, at S-band only about 5 dipoles per meter could be placed in the ribbon or 50 dipoles for a 10 m ribbon length giving a radar cross-section of .086 m^2 per ribbon. This would necessitate that 116 of the ribbons would have to be used to add 10 m^2 to the cross-section of the iceberg of Fig. 4-1. The enhanced cross-section , σ_e, of the iceberg would be:

$$\begin{aligned} \sigma_e &= \sigma_i + \sigma_n \\ &= 0.0142\,A + 10 \\ &= 3.2 + 10 \\ &= 13.2\ m^2 \end{aligned} \qquad (4.4)$$

where

σ_i is the iceberg radar cross-section
σ_n is the new radar cross-section
A is the projected area of the iceberg in Fig. 4-1 (approx. 225 m^2)

This is equivalent to a 6 dB increase in radar cross-section (i.e. σ_i (dB) = 10 log (3.2) = 5.1 dB and σ_e (dB) = 10 log (13.2) = 11.1 dB for a 6 dB increase). A 3 dB increase in cross-section would require 37 ribbons.

The second alternative to the standard chaff would be to use much more rigid dipoles, rigid chaff, and a launching device which would force the dipoles to penetrate the iceberg surface. The whole iceberg face would be peppered with these dipoles which would provide similar cross-section enhancements to the ribbon.

Both of these methods or techniques would require good penetration into the iceberg surface to ensure the anchoring pins for the ribbon and the dipoles themselves for the second method could withstand at least several days of iceberg melting and weathering.

The main problems associated with these techniques are:

1. Deployment: Even for a modest 3 dB increase in radar cross-section on a small iceberg, 37 chaff ribbons would have to be deployed on each face of the iceberg requiring 148 ribbons per iceberg. Individual deployment of the ribbons would be time-consuming using a line throwing gun approach, however, this may be overcome by

the possible grouping of a number of ribbons in one deployment package. With the careful design of the deployment package, it is expected that a high success rate could be achieved.

The deployment of rigid chaff into an iceberg face poses a much more difficult problem. It is necessary to have the dipoles penetrate far enough into the iceberg such they are not immediately washed off by iceberg melt water. Penetration of several inches may be enough to prevent this and if the dipoles absorb sufficient radiant energy, it is possible that they will continue to melt into the iceberg faster than the ablation of the iceberg. Deployment of several hundred of these dipoles could be accomplished using a shotgun type shell package to hold them (approximate dipole size is 4.55 cm long with a 0.12 cm diameter for S-band and 1.46 cm long with a 0.04 cm diameter for X-band).

2. Iceberg rolling: Depending on the amount of roll, these methods may be rendered useless.

3. Iceberg melting: Iceberg melting will, to some extent, control the useful life of these techniques as sooner or later the anchoring pins and chaff dipoles will fall free from the icebergs. Depending on the threat an iceberg poses, several hours of enhanced detection may be sufficient. The effect of melting around the anchoring pins may be minimized by designing a delivery system which will break away leaving a metal dart anchor under the ice surface secured to the chaff ribbon by nylon or kevlar cord. The rigid chaff should be chosen to maximize its absorption of radiant thermal energy. This will ensure the chaff will melt into the iceberg face.

II) Reflective mesh:

An alternative to the use of chaff ribbon is to use a reflective mesh which could be deployed using the dart and gun method mentioned earlier. The net may be cut to any desired width and its weight would permit easy deployment (18 g/m^2 for Chemring 1022 radar mesh - see Appendix 3 for specifications). With several strips of this mesh secured to the iceberg it is expected that at least some portion of the mesh will point toward the radar. As its reflectivity is quoted at 0.95 its radar cross-section should approach that of steel plate of modest size. If, for example, a 20 cm wide strip of mesh 5 m long was deployed on the iceberg and only a 10 cm length was pointed at the radar then the radar cross-section of that portion of the mesh (20 cm x 10 cm)

would be 5 m^2 giving a 3 dB enhancement of the cross-section for the iceberg of Fig. 4-1. It is expected that there would be more than one mesh area pointed in the direction of the radar and in addition the segments that are pointed in other directions will also contribute to the overall cross-section, although to a lesser degree. The deployment of these strips of mesh could be accomplished fairly easily with a dart and gun assembly and a high degree of success is expected.

III) Off-berg reflectors:

Several types of reflectors may be utilized from standard radar reflectors to reflector kites and reflector carrying balloons. Each of these methods will rely on a mooring technique utilizing a dart anchor with tether line to the reflector. The selected airborne reflectors have the advantage over the standard corner reflector type, both in their ability to produce a larger cross-section for the same weight (due to the use of light weight material) and their altitude advantage, giving longer tracking ranges than surface borne reflectors.

Light weight corner reflectors attached to a balloon have been successfully used for meteorological studies. A reflector with a 1.37 m size (see Fig. 4-2) will provide a radar cross-section of about 2000 m2 at X-band and about 200 m2 at S-band (specifications provided in Appendix 3). Targets of these radar cross-sections would effectively overpower the cross-section of the iceberg to which it was attached. This reflector configuration would be susceptible to wind drag on the balloon and in high wind area it may be better to use similar size reflectors fabricated from aluminum coated mylar and fashioned into a box kite form. (See Fig. 4-3.) This type of radar reflector kite was patented by F.M. Rogallo in 1967 (Greger, 1984) and its box kite configuration will provide a stable target even in high wind. The radar cross-section of the two cell kite of Fig. 4-3 would be about 2000-3000 m^2 at X-band and about 200-300 m^2 at S-band.

The air launching of either the balloon/reflector combination or the kite could be accomplished from a support vessel once the anchor dart has been secured to the iceberg.

The choice of balloon or kite reflector will depend on the prevailing wind conditions. With a wind above 10 knots a kite will provide a reliable steady target and for less than 10 knots a balloon/reflector combination may be used.

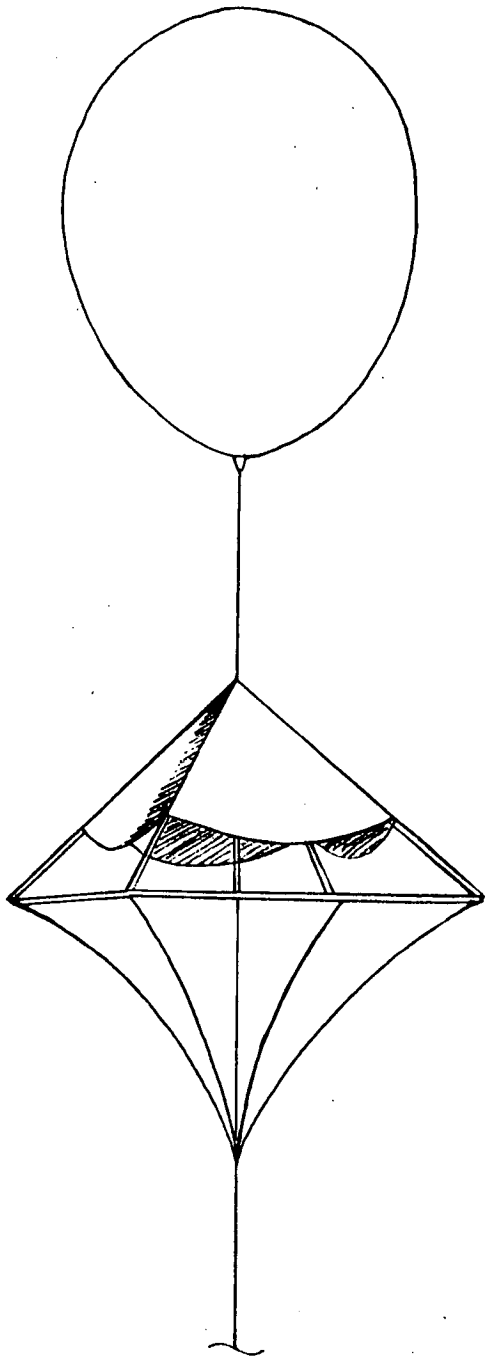

Fig. 4-2. Balloon supported radar reflector.

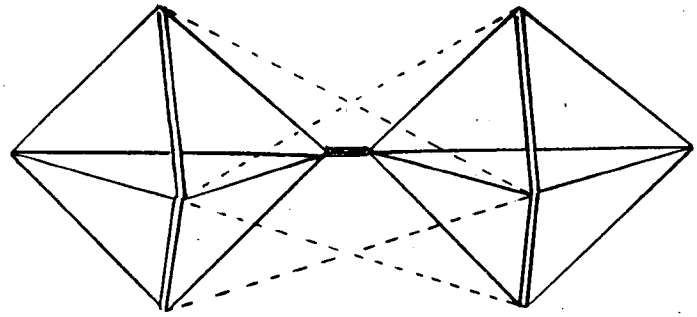

Fig. 4-3. Two cell Rogallo corner kite.

4.2 ACTIVE METHODS

While active methods do not fall strictly in the category of enhancement techniques, they will certainly extend the tracking range beyond that which could be expected under normal operations. Each of the active techniques proposed here will use the same type of mooring system. Essentially a floating buoy will house the required instrument package. This buoy will be tethered to the iceberg using a dart and line method similar to that demonstrated by Robe (1978). This method of mooring reduces some of the problems associated with iceberg rolling and melting. Calving will still cause some problems for this type of system.

I) Radar transponder:

The radar transponder package will consist of an X-band radar transponder similar to that marketed by Motorola (specifications provided in Appendix 3) along with a power supply and mooring system described above. The transponder is essentially a radar unit which transmits a delayed coded pulse response when interrogated by a radar operating on the transponders receiver frequency. Loss of the transponder signal may occur if the iceberg gets between the transponder and the interrogating radar. The power supply will have sufficient capacity to permit transponder operation for a three-day period (arbitrary based on desired tracking time). The reliable (100%) tracking range of this type of unit will be governed by the radar horizon as calculated by:

$$R(km) = \sqrt{17\ h_a} + \sqrt{17\ h_t} \qquad (4.5)$$

where

R = range to horizon (km)
h_a = radar antenna height (m)
h_t = transponder height (m)

Typical units of this value will cost in the vicinity of $20,000 plus the cost of the power supply/buoy package. (Probable total cost of $25,000 per complete package.)

II) Radio direction finder:

The radio direction finder concept for iceberg tracking has been used with limited success by Hayes in 1974 to track icebergs, Robe (1977). The instrument package in this case would consist of a basic radio transmitter operating at a set frequency. The position of the package may then be located in range and bearing using a two site direction finding system as illustrated in Fig. 4-4.

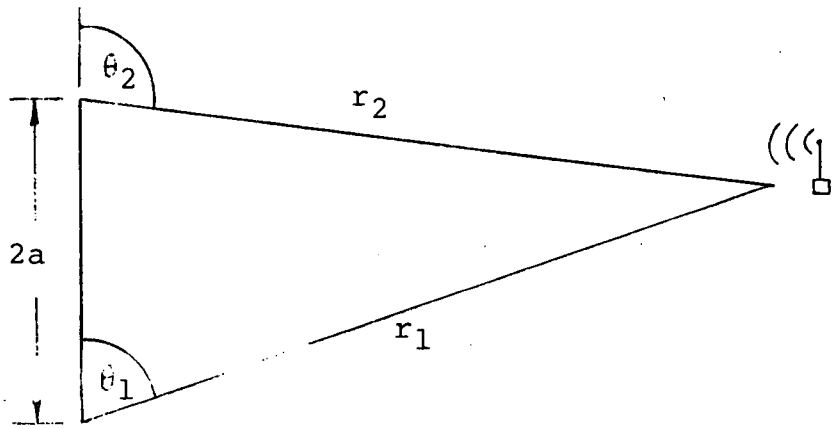

Fig. 4-4. Geometry for a two-site direction finding system.

The range and bearing from either platform of Fig. 4-4 may then be calculated by using the formula,

$$r_1 = \sqrt{(x+a)^2 + y^2}\ ,\ r_2 = \sqrt{(x-a)^2 + y^2} \qquad (4.6)$$
$$\theta_1 = \tan^{-1}(y/x+a)\ ,\ \theta_2 = \tan^{-1}(y/x-a)$$

Where

$$x = a\,\frac{\sin(\theta_1+\theta_2)}{\sin(\theta_1-\theta_2)}$$
$$y = a\,\frac{\sin\theta_1 \sin\theta_2}{\sin(\theta_2-\theta_1)}$$

Specifications for a typical direction finding system are contained in Appendix 3. The advantage of this type of system is that direction finding equipment is frequently installed as standard equipment on drilling platforms and support vessels and the transmitter used with the system can be a very inexpensive HF (High Frequency) unit. With proper selection of operating frequency tracking, ranges in excess of 100 naut mi are expected (see Appendix 4 for discussion).

III) LORAN retransmission system:

A unit capable of similar range performance would utilize a LORAN or other navigation system to locate itself then transmit this position information to a base station. This type of system is easily automated with the base station polling each unit at selected intervals and updating a positional display containing present position and status of the units (icebergs). Harwood (1971) had suggested this type of system for iceberg tracking and indicated that the system was the subject of a contract with Marconi. Marconi Canada presently markets a Vehicle Traffic Management System based on the use of LORAN C with user selectable retransmission packages available for VHF and HF frequencies. This system would also be very useful for tracking support vessels.

IV) HF radar transponders:

An alternative to the microwave transponder would be to use transponders operating in the HF frequency band (3-30 MHz). These transponders, when utilized with existing HF radar systems (for example CODAR), can provide very accurate radial velocity measurements on the order of 1 mm/sec with range positional accuracy better than 50 m. While it would be necessary to have a two site CODAR to derive velocity vectors (i.e. two radial components from separated sites are required), only one site would be required for tracking as CODAR uses a direction finding technique to calculate the angle of arrival of the transponder signal. Experiments by Gulf Oil Exploration and Production Company in the Arctic have demonstrated the tracking of 25 transponders simultaneously. The maximum operating range reported by Crissman (1985) with this system was about 60 km (32.4 naut mi) and this was for a path that was part open sea and part sea ice. Over open ocean a maximum operating range of 76.8 km (41.5 naut mi) can be expected with CODAR.

While the HF transponders themselves are relatively inexpensive (about $1,500), the cost of an HF radar system

would be a major expense (approximately $150,000 for a single site system plus installation). The feasibility of detecting icebergs with HF radar has been demonstrated (Walsh, et. al. 1985) and HF systems such as CODAR are already used operationally to obtain ocean surface current. It is possible that the performance of HF radar for iceberg detection will nullify the need to use a transponder.

V) Satellite tracking:

A final alternative would be the use of satellite tracking systems presently in operation. The service ARGOS system has been used successfully to track meteorological buoys and balloons. Petro-Canada has recently used the Service ARGOS System to monitor ice movement. The system is primarily used as a research tool and it is expected that the service will be available through to 1990.

The platform terminal transmitter located on buoy can accept data from 32 sensors and transmit the data to the ARGOS satellite system. For the Grand Banks region, updates of position and data are available through the ARGOS network about twice daily. Alternatively the user can operate a direct receiver facility that will receive the platform data as the satellite passes over the coverage area. The direct receiver facility will provide a coverage area having a radius of about 2500 km with about 12 position fixes per 24 hours at 45° latitude. Positional accuracy for buoy location is estimated to be no worse than $\pm$1 km and is typically $\pm$250 m.

5. EVALUATION OF THE TECHNIQUES

In the following Chapter the proposed enhancement techniques are evaluated. The passive techniques are evaluated in terms of increased detection range and the active techniques are presented with reference to their maximum operational ranges.

The passive enhancement of the detectability of icebergs may be assessed by comparing the present detection capability for several icebergs in different sea conditions with the improvement that can be achieved by enhancing the target.

Figs. 5-1 through 5-6 present the detectability of three iceberg sizes in sea state 5 (SWH = 2.5 m) using six alternate enhancement techniques. The techniques are classified as:

a) Chaff

Chaff filaments in either ribbon, rigid or conventional configuration.

For radar cross-section of 5 m^2 at X-band, 28,400 filaments are required and at S-band 2,900 filaments are required.

For radar cross-section of 10 m^2 at X-band, 56,800 filaments are required and at S-band, 5,800 filaments are required.

b) Reflective mesh

For a radar cross-section of 10 m2 at X and S Bands, two 5 m lengths of 20 cm wide mesh are required.

c) Reflective balloon

A spherical balloon with a highly reflective mesh cover. For a 1 m diameter, its radar cross-section will be about 3 m2 at both X- and S-band. The height of the balloon will depend on line length, line weight, balloon drag and wind conditions. A 20 m height is assumed for this analysis.

d) Balloon/corner reflector

A balloon with a suspended corner reflector having a 2000 m^2 radar cross-section at X-band and a 200 m^2

radar cross-section at S-band. A reflector height of 20 m is selected for analysis.

e) Rogallo corner kite

Rogallo design box kite made from aluminum coated mylar. Double corner design will provide 2000 - 3000 m^2 cross-section at X-band and 200 - 300 m^2 at S-band. Approximate physical size 1 m x 1 m x 2 m. A kite height of 50 m is selected for analysis.

f) Buoy/reflector

Conventional buoy with attached radar reflector having a radar cross-section of about 500 m^2 at X-band and 50 m^2 at S-band.

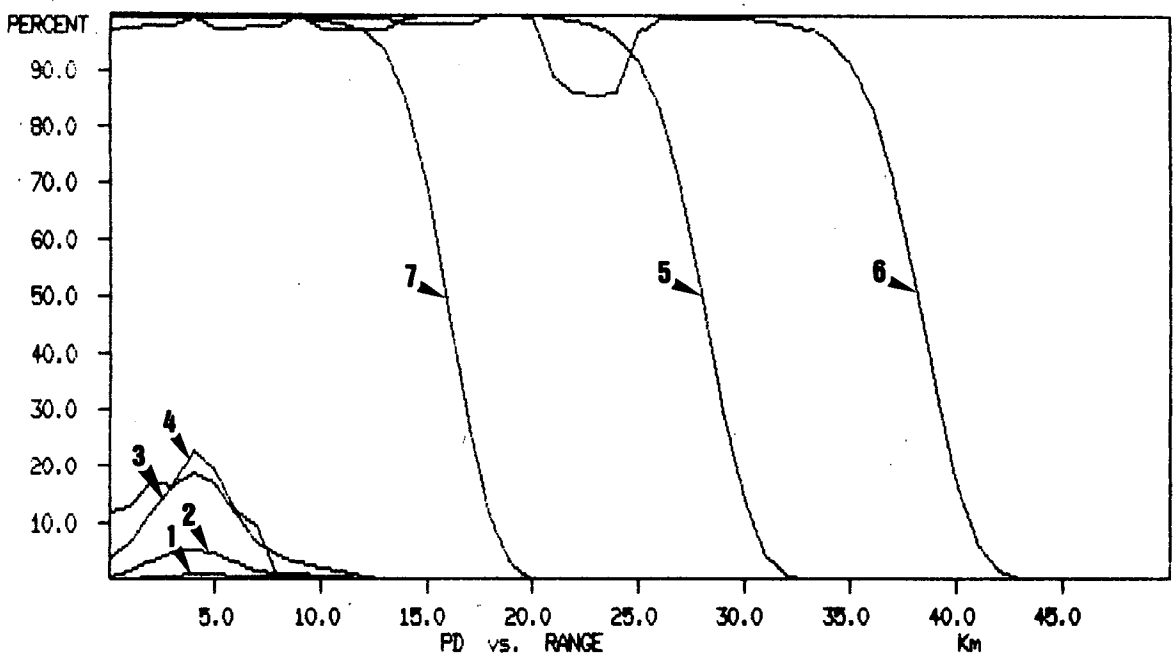

Frequency = X-band
Antenna height = 15 m
Pulse length = 1.0 μsec

Curve 1 - unenhanced 4 x 10 x 10 m (above water) iceberg
Curve 2 - 3 dB enhancement with chaff or reflective mesh
Curve 3 - 6 dB enhancement with chaff or reflective mesh
Curve 4 - reflective balloon
Curve 5 - balloon/reflector
Curve 6 - Rogallo corner kite
Curve 7 - buoy/corner reflector

Fig. 5-1. Probabilities of detection for a bergy bit in a 2.5 m (significant wave height) sea with and without passive enhancement for X-band.

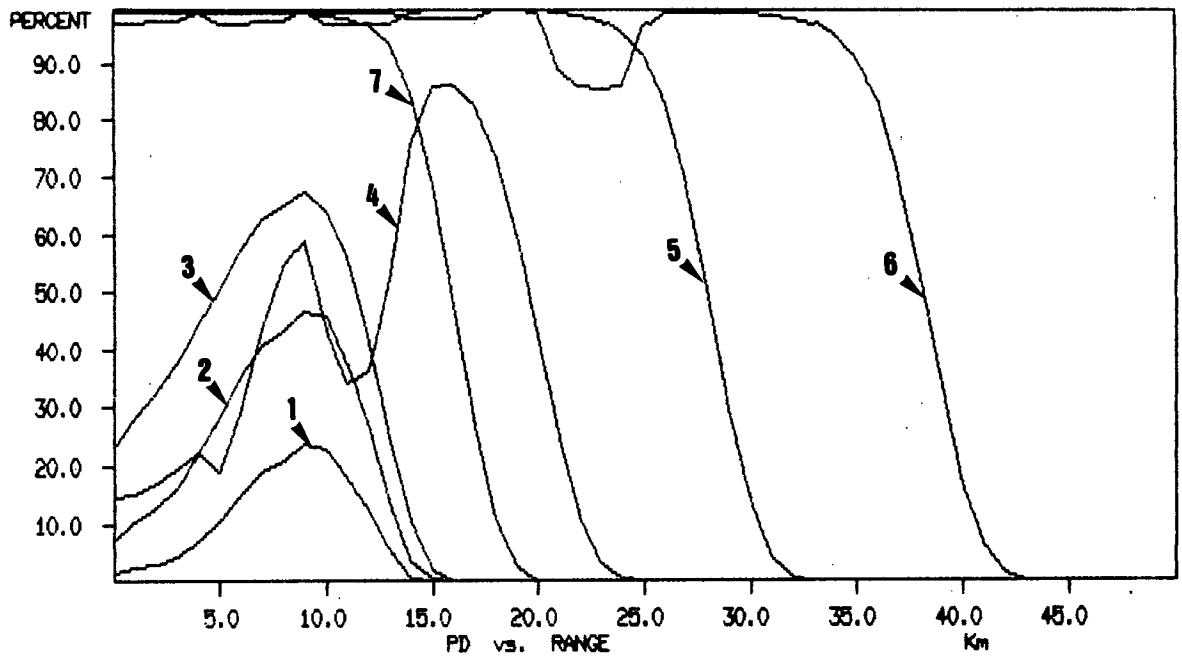

Frequency = X-band
Antenna height = 15 m
Pulse length = 1.0 μsec

Curve 1 - unenhanced 7 x 10 x 10 m (above water) iceberg
Curve 2 - 3 dB enhancement with chaff or reflective mesh
Curve 3 - 6 dB enhancement with chaff or reflective mesh
Curve 4 - reflective balloon
Curve 5 - balloon/reflector
Curve 6 - Rogallo corner kite
Curve 7 - buoy/corner reflector

Fig. 5-2. Probabilities of detection for a small iceberg in a 2.5 m (significant wave height) sea with and without passive enhancement for X-band.

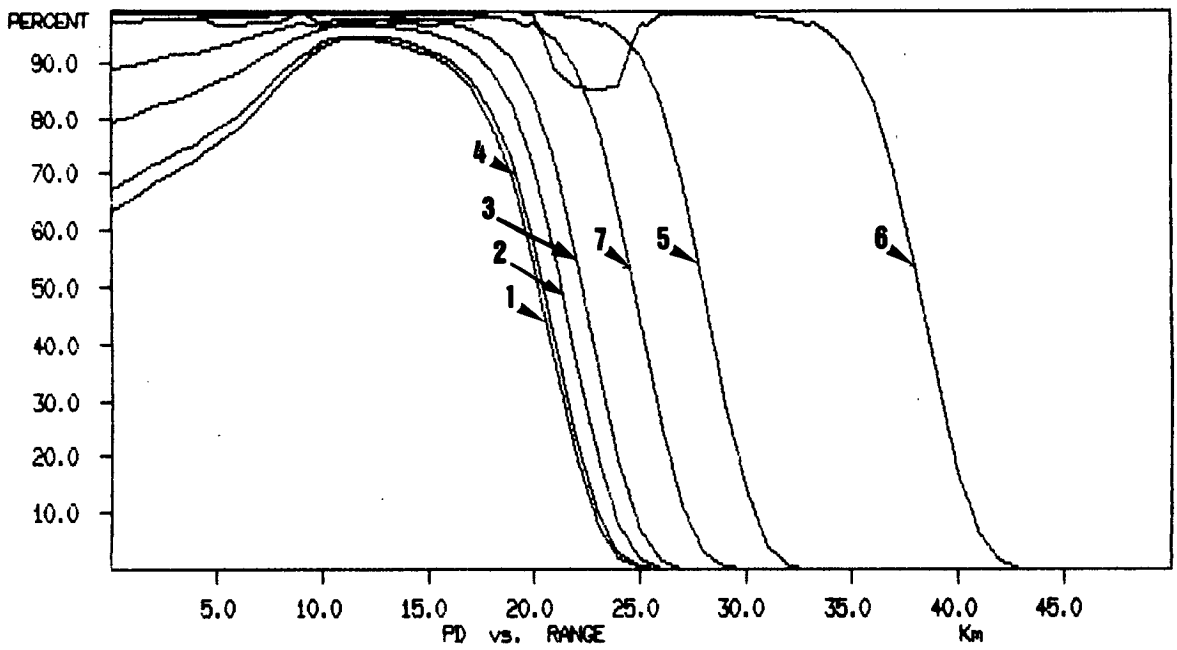

Frequency = X-band
Antenna height = 15 m
Pulse length = 1.0 μsec

Curve 1 - unenhanced 25 x 60 x 60 m (above water) iceberg
Curve 2 - 3 dB enhancement with chaff or reflective mesh
Curve 3 - 6 dB enhancement with chaff or reflective mesh
Curve 4 - reflective balloon
Curve 5 - balloon/reflector
Curve 6 - Rogallo corner kite
Curve 7 - buoy/corner reflector

Fig. 5-3. Probabilities of detection for a medium iceberg in a 2.5 m (significant wave height) sea with and without passive enhancement for X-band.

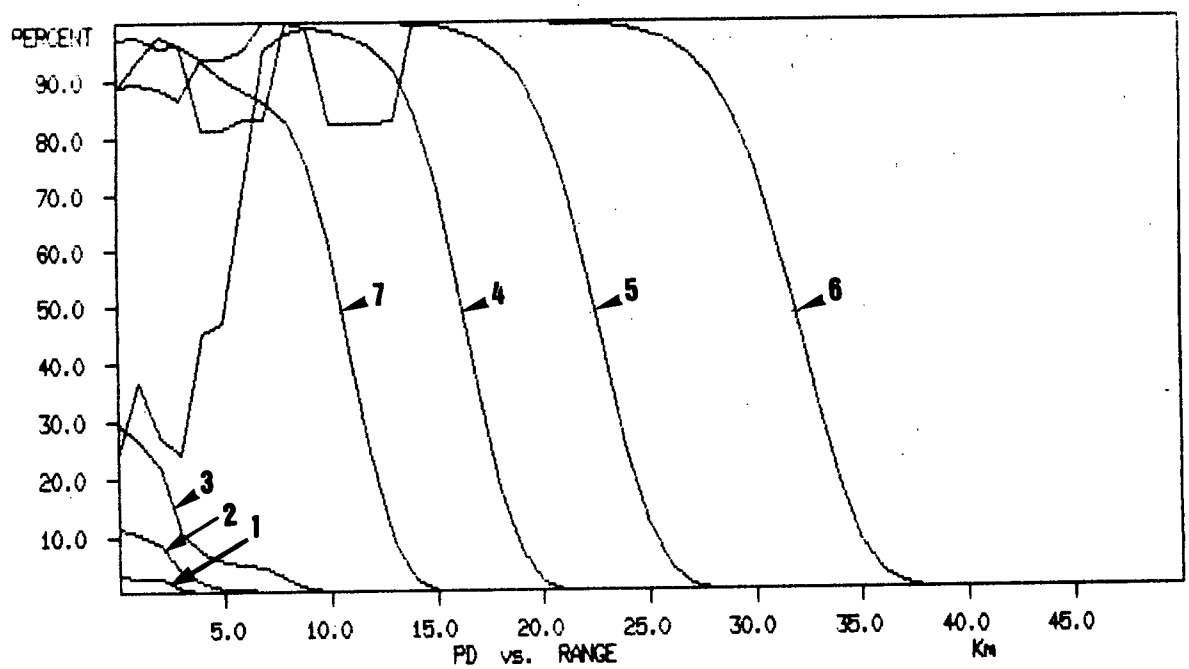

Frequency = S-band
Antenna height = 15 m
Pulse length = 1.0 μsec

Curve 1 - unenhanced 4 x 10 x 10 m (above water) iceberg
Curve 2 - 3 dB enhancement with chaff or reflective mesh
Curve 3 - 6 dB enhancement with chaff or reflective mesh
Curve 4 - reflective balloon
Curve 5 - balloon/reflector
Curve 6 - Rogallo corner kite
Curve 7 - buoy/corner reflector

Fig. 5-4. Probabilities of detection for a bergy bit in a 2.5 m (significant wave height) sea with and without passive enhancement for S-band.

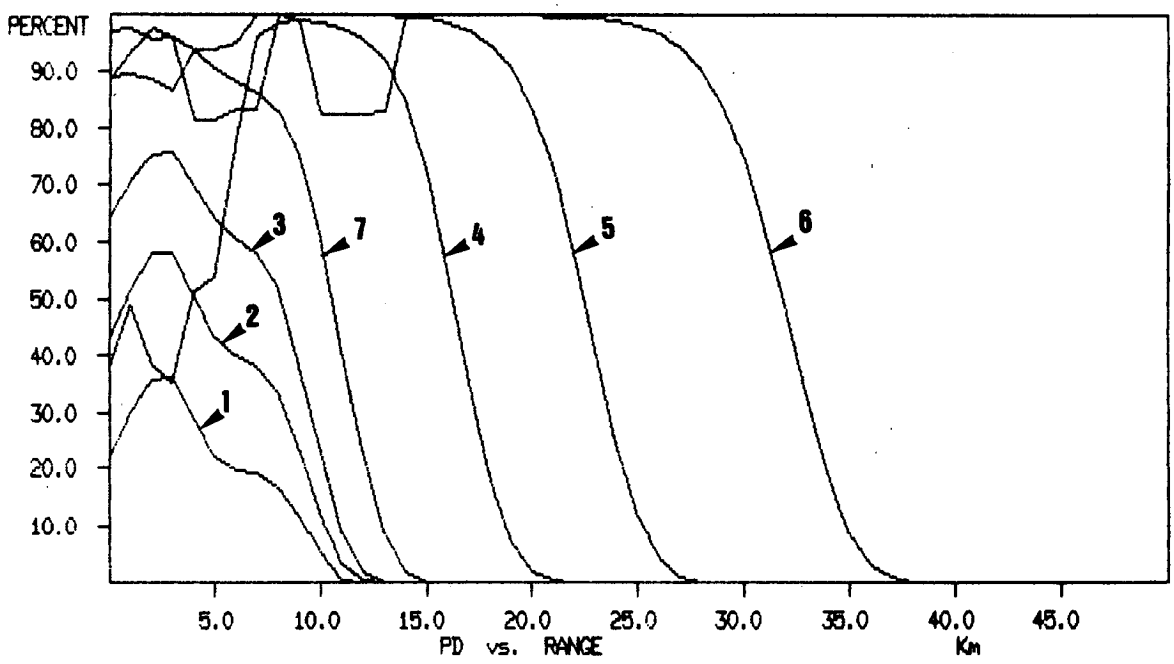

Frequency = S-band
Antenna height = 15 m
Pulse length = 1.0 μsec

Curve 1 - unenhanced 7 x 10 x 10 m (above water) iceberg
Curve 2 - 3 dB enhancement with chaff or reflective mesh
Curve 3 - 6 dB enhancement with chaff or reflective mesh
Curve 4 - reflective balloon
Curve 5 - balloon/reflector
Curve 6 - Rogallo corner kite
Curve 7 - buoy/corner reflector

Fig. 5-5. Probabilities of detection for a small iceberg in a 2.5 m (significant wave height) sea with and without passive enhancement for S-band.

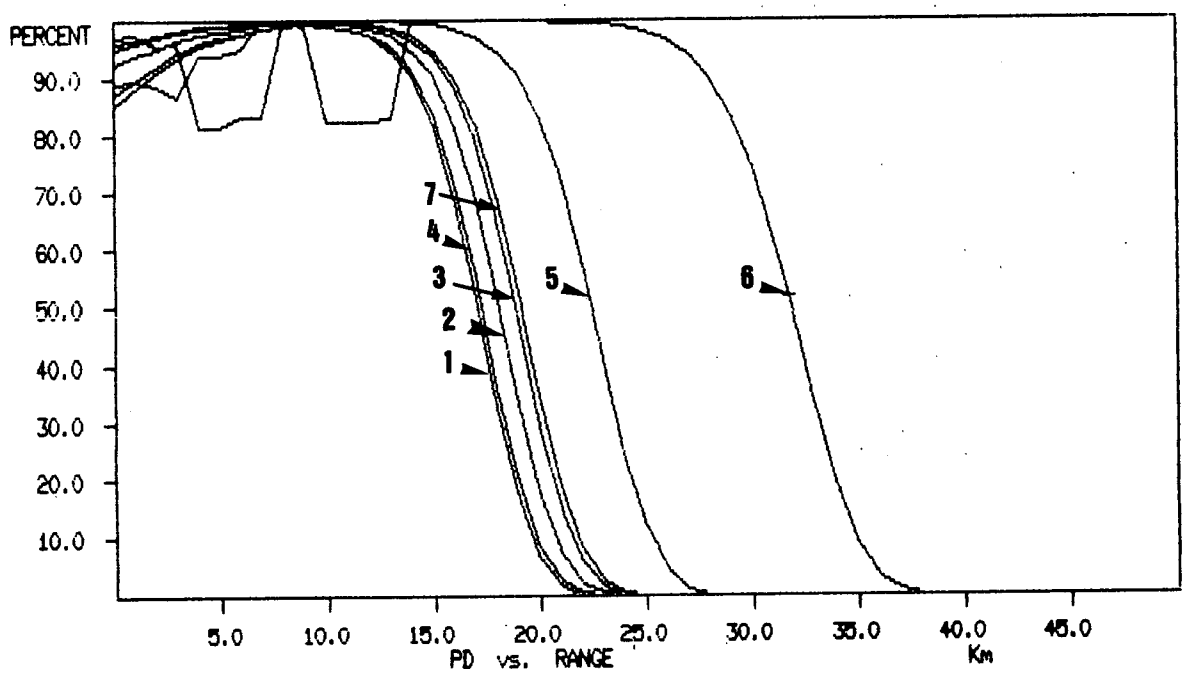

Frequency = S-band
Antenna height = 15 m
Pulse length = 1.0 μsec

Curve 1 - unenhanced 25 x 60 x 60 m (above water) iceberg
Curve 2 - 3 dB enhancement with chaff or reflective mesh
Curve 3 - 6 dB enhancement with chaff or reflective mesh
Curve 4 - reflective balloon
Curve 5 - balloon/reflector
Curve 6 - Rogallo corner kite
Curve 7 - buoy/corner reflector

Fig. 5-6. Probabilities of detection for a medium iceberg in a 2.5 m (significant wave height) sea with and without passive enhancement for S-band.

From Figs. 5-1 to 5-6 it is clear that the reflector approach, whether it be buoy mounted or balloon mounted, will provide superior performance over the chaff enhancement techniques.

The chaff loads considered in the previous analysis are actually quite modest representing probably the minimum improvement which could be obtained. With careful design of the chaff and deployment method, it should be possible to achieve greater enhancement.

The kite and balloon/reflector combinations will provide the most reliable enhancement as they will not be subject to wave motion and obscuration which would effect the buoy mounted reflector. The results of Figs. 5-1 to 5-6 are summarized along with expected costs and operational considerations and presented in Table 5-1.

The active techniques may be considered in terms of their performance. Table 5-2 lists the systems as presented in Chapter 4 providing the operational capabilities and approximate cost of each. These systems will be deployed with a dart and line tethering approach similar to that used by Robe (1978) and Diemand (1984). The instrument package would be located on a floating buoy tethered to the iceberg.

Table 5-2 indicates that the Radio Direction Finder (RDF) technique would probably be the most cost effective technique provided direction finding equipment is already installed (RDF equipment is available on some offshore supply vessels and rigs). This technique has the added complexity over the other techniques of Table 5-2 in that two separated receivers are required. This may not pose much of a problem if say a rig and its support vessel have RDF equipment. Another minor complication with this system would be the tracking of a number of different RDF beacons. In this case either a method of interrogating the beacons would be used or each beacon could operate on a different frequency (may be a problem in frequency allocation). The X-band radar transponder has the highest unit cost and the shortest range performance (about 44 km for a derrick mounted X-band interrogating radar). The HF transponder has a much lower unit cost, however, the HF radar system cost is high. The HF transponder method may become the most feasible should HF radars be used operationally for ocean monitoring and iceberg detection from offshore platforms.

For overall system independence (i.e. single site), cost and performance the LORAN retransmission package

TABLE 5-1

Passive enhancement techniques.

Type	Est. cost per iceberg $	Enhancement on small icebergs (dB)	Detection range for an enhanced 7 x 15 x 15 iceberg in 2.5 m SWH (Not detected on either X- or S-band long pulse) (km)
Chaff	50.0	3 - 10 dB	6-12 km for 6 dB enhancement (X-band) 8 km for 6 dB enhancement (S-band)
Reflective mesh	200.0	3 - 10 dB	6-12 km for 6 dB enhancement (X-band) 8 km for 6 dB enhancement (S-band)
Reflective balloon	250.0	4 - 6 dB	7-20 km (X-band) 17 km (S-band)
Balloon/ corner reflector	250.0	30 dB	27 km (X-band) 23 km (S-band)
Rogallo corner kite	350.0	32 dB	37 km (X-band) 32 km (S-band)
Buoy/ corner reflector	500.0	25 dB	16 km (X-band) 16 km (S-band)

TABLE 5-2

Comparison of active tracking/enhancement methods.

Technique	Operational range (km)	Position of accuracy (m)	Deployment	Cost	Operational considerations
Radar transponders:					
X-band	$\sqrt{17\ h_a} + \sqrt{17\ h_t}$ [1]	R=±30, = ±1°	Buoy & tether line to anchor dart on berg	25K/unit + radar (standard)	Power supply required + environmental housing.
HF	75 (CODAR)	±50		3 K/unit + radar (150 K)	
Radio direction finder/beacon	180	±2° ±3500 at 100	Buoy & tether line to anchor dart on berg	3 K/unit + radio direction finder (available on most offshore vessels and rigs).	Two separated receivers required for range and bearing calculation (i.e. two ships or ship and rig)
LORAN retransmission	180	±300	Buoy & tether line to anchor dart on berg	6 K/unit base station (40K)	Up to 256 units may be tracked.
Satellite (ARGOS)	2500	±1000	Buoy & tether line to anchor dart on berg	6 K/unit + direct receiver facility (35K)	Presently experimental type projects. Only 12 passes per day. Dependent on ARGOS system.

[1] h_a = antenna height (m)
h_t = transponder height (m)

(see Appendix 3) may provide the best alternative. The system is configured to track up to 256 units and is capable of receiving status information from each. This system would be useful in providing support vessel and aircraft tracking as well.

The use of the Service ARGOS system is a viable alternative provided instantaneous positioned information is not required. With satellite passes averaging about 12 per day in the Hibernia area, it would only be possible to have position updates every two hours.

6. CONCLUSIONS AND RECOMMENDATIONS

A study has been carried out to investigate the use of enhancement techniques to increase the radar detectability of icebergs. The proposed techniques are grouped in two categories; namely, passive and active. The passive techniques include the use of various types of radar reflective material deployed on the iceberg as well as reflective balloons, balloon and reflector combinations and radar reflector kites. The active techniques include the use of radar transponders, radio direction finders, radio navigation systems and satellite tracking systems.

The passive enhancement techniques described should provide reliable short-term increases in the radar detection of icebergs. These techniques, especially those deployed on the icebergs, will only enhance detection within the radar horizon. The use of reflective balloons, balloon reflector combinations and reflector kites will extend the detection horizon for a particular iceberg. The highest probability of detection will be achieved using the balloon-mounted reflector and reflector kite. These systems are complimentary with the kite being better suited to windy conditions and the balloon/reflector to calm conditions.

The active techniques considered will all provide reliable detection within their operational range. The satellite tracking system would offer the largest tracking range (about 2500 km) with position updates about every two hours. The LORAN retransmission system will provide the longest range performance (about 180 km) of the stand alone (i.e. full receiver package located at one base station) system. The radio direction finder will offer similar range performance to the LORAN system with the added complexity of requiring that the signal be received from two separated sites in order to calculate range and bearing. The HF radar transponder offers the next longest range performance of about 75 km. This 75 km range limitation is imposed by the existing CODAR design and may be increased considerably. With the use of alternate frequencies and different radar parameters this range could be extended. The X-band radar transponder is perhaps the most limited in performance providing not much more than the normal radar horizon. These units are also the most expensive with their only real advantage being in their superior positional accuracy.

Finally, it is recommended that the passive techniques identified be subjected to field trials. These

techniques might be evaluated at relatively minor cost considering the results presented in Table 5-1. The long range tracking systems considered under the active category should be evaluated in terms of operational requirements. Deployment methods should be investigated with specific attention to the dart and line methods proposed for the tethered buoy and airborne passive techniques.

Appendix 1

Propagation Factor for a Flat Smooth Sea

Propagation Factor for a Smooth Flat Sea

The detection of height extensive targets at sea is influenced by the effect of multipath propagation. Multipath propagation occurs in both the forward (radar to target) and reverse (target to radar) directions. The geometry of the problem is given in Figure A1-1. It is useful to consider the simplified case of propagation over a smooth flat sea in order to gain insight into the more complex problem of propagation over a rough spherical earth.

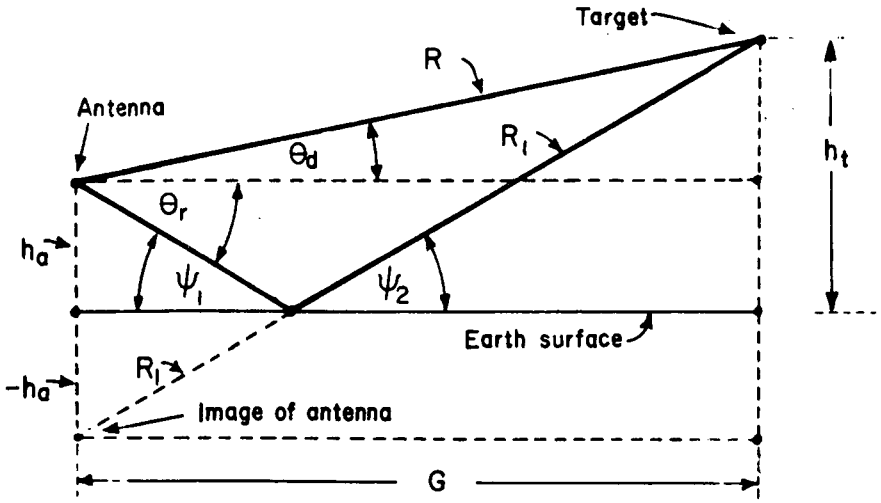

Fig. A1-1. Geometry of Multipath Problem for Propagation Over a Smooth Flat Sea.

From the geometry of Figure A1-1 we have,

$$R^2 = (h_a - h_t)^2 + G^2 \qquad (1)$$

$$R_1^2 = (h_t + h_a)^2 + G^2 \qquad (2)$$

Substituting G^2 from (1) into (2) yields

$$R_1 = (4h_a h_t + R^2)^{1/2} \qquad (3)$$

The important quantity in the multipath calculation is the path length difference, δ , between the direct path, R, and the reflected path, R_1, and is given by,

$$\delta = R_1 - R$$
$$\delta = (4h_a h_t + R^2)^{1/2} - R \qquad (4)$$

Now for

$$4h_a h_t << R^2 \tag{5}$$

we may use a Taylor Series expansion about R^2 yielding

$$(4h_a h_t + R^2)^{1/2} \simeq R + \frac{4h_a h_t}{2R} - \frac{1}{4}\frac{(4h_a h_t)^2}{2^1 R^3} + \ldots$$

which may be approximated by

$$(4h_a h_t + R^2)^{1/2} \simeq R + \frac{4h_a h_t}{2R} \tag{6}$$

and the path length difference is given as,

$$\delta = R_1 - R \tag{7}$$

$$\delta = \frac{2h_a h_t}{R}$$

Using this expression for δ the propagation factor is given by,

$$F^2 = 1 + P^2 - 2P \cos (4\pi h_a h_t/\lambda R) \tag{8}$$

Where P is the reflection coefficient of the sea
λ is the radar wavelength
F^2 is the propagation factor

For a flat smooth sea P may be approximated by unity giving,

$$F^2 = 2(1-\cos (4\pi h_a h_t/\lambda R)) \tag{9}$$

Integrating equation (9) over the height of the target, h_t, yields,

$$\int_0^{h_t} F^2 dh = 2h_t - \frac{\lambda R}{2\pi h_a} \sin \left\{ \frac{4\pi h_a h_t}{\lambda R} \right\} \tag{10}$$

and the average propagation factor over the height of the target is

$$(F^2)_{av} = \frac{1}{h_t} \int_0^{h_t} F^2 dh = 2 - \frac{\lambda}{2 h_a h_t} \sin \left\{ \frac{4\pi h a h t}{\lambda R} \right\}$$

$$= 2 \left\{ 1 - \frac{\sin x}{x} \right\} \tag{11}$$

where

$$x = \frac{4\pi h_a h t}{\lambda R} \tag{12}$$

The propagation factor of equation (11) relates the electric field strength due to multipath to the field strength that would be present if no multipath occurred. Since the power received by a radar is proportional to the electric field strength squared, the propagation factor that occurs in the radar equation (see equation (3.2) in section 3.1) will be,

$$F^4 = ((F^2)_{av})2$$

$$= 4\left\{1-\frac{\sin x}{x}\right\}^2 \qquad (13)$$

where x is given in equation (12).

For large x the propagation factor in (13) will be on average about 4 which would yield a 6 dB increase in received signal power. The actual propagation factor over a rough spherical sea is expected to be less than this especially for a very rough sea. In a calm sea at close ranges, the propagation factor will approach that given by equation (13) and therefore should be taken into account when either calculating received power or radar cross section.

Appendix 2

Curves for Present Detection Capability

Index of Probability of Detection Plots

Figure	Band	Antenna Height	SWH	Pulse Length
A-1	X	15 m	0.5 m	1.0 μsec
A-2	X	15 m	0.5 m	0.25 μsec
A-3	X	75 m	0.5 m	1.0 μsec
A-4	X	75 m	0.5 m	0.25 μsec
A-5	X	15 m	2.5 m	1.0 μsec
A-6	X	15 m	2.5 m	0.25 μsec
A-7	X	75 m	2.5 m	1.0 μsec
A-8	X	75 m	2.5 m	0.25 μsec
A-9	X	15 m	5.0 m	1.0 μsec
A-10	X	15 m	5.0 m	0.25 μsec
A-11	X	75 m	5.0 m	1.0 μsec
A-12	X	75 m	5.0 m	0.25 μsec
A-13	S	15 m	0.5 m	1.0 μsec
A-14	S	15 m	0.5 m	0.25 μsec
A-15	S	75 m	0.5 m	1.0 μsec
A-16	S	75 m	0.5 m	0.25 μsec
A-17	S	15 m	2.5 m	1.0 μsec
A-18	S	15 m	2.5 m	0.25 μsec
A-19	S	75 m	2.5 m	1.0 μsec
A-20	S	75 m	2.5 m	0.25 μsec
A-21	S	15 m	5.0 m	1.0 μsec
A-22	S	15 m	5.0 m	0.25 μsec
A-23	S	75 m	5.0 m	1.0 μsec
A-24	S	75 m	5.0 m	0.25 μsec

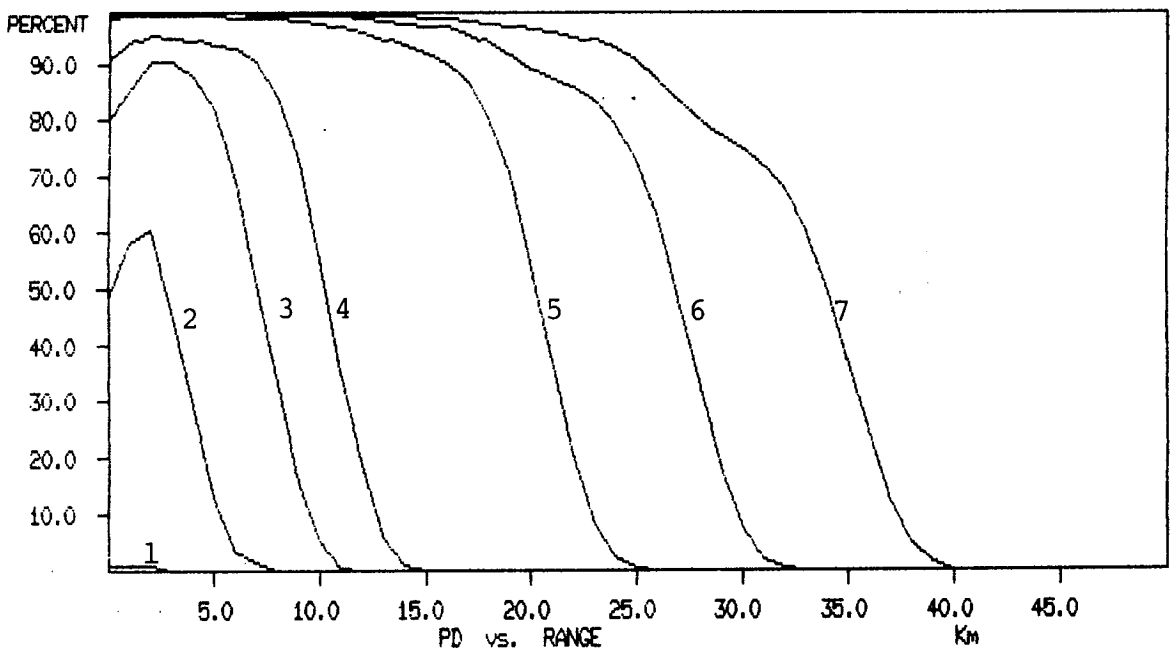

Antenna Height		15 m
Significant Wave Height		0.5 m
Pulse Length		1.0 μsec
Curve 1	Iceberg	1 m x 1 m x 1 m
Curve 2	Iceberg	2 m x 5 m x 5 m
Curve 3	Iceberg	4 m x 10 m x 10 m
Curve 4	Iceberg	7 m x 15 m x 15 m
Curve 5	Iceberg	25 m x 60 m x 60 m
Curve 6	Iceberg	45 m x 110 m x 110 m
Curve 7	Iceberg	75 m x 170 m x 170 m

Fig. A-1. Probability of detection for an X-Band radar.

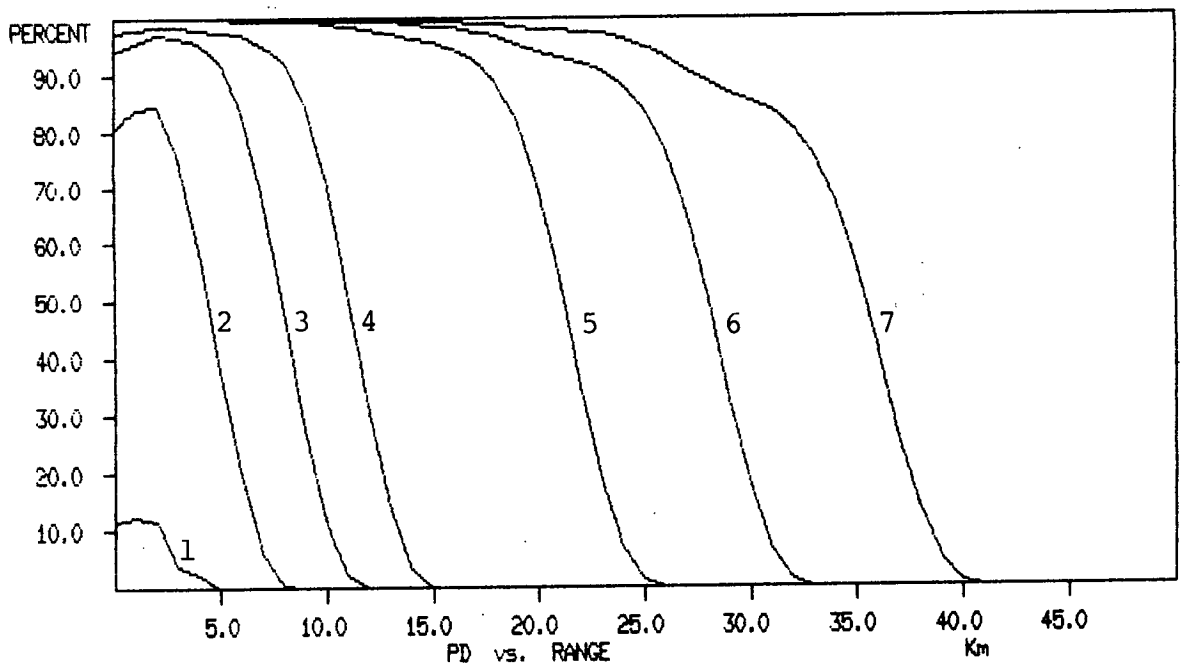

Antenna Height	15 m
Significant Wave Height	0.5 m
Pulse Length	0.25 μsec

Curve 1	Iceberg	1 m x 1 m x 1 m
Curve 2	Iceberg	2 m x 5 m x 5 m
Curve 3	Iceberg	4 m x 10 m x 10 m
Curve 4	Iceberg	7 m x 15 m x 15 m
Curve 5	Iceberg	25 m x 60 m x 60 m
Curve 6	Iceberg	45 m x 110 m x 110 m
Curve 7	Iceberg	75 m x 170 m x 170 m

Fig. A-2. Probability of detection for an X-Band radar.

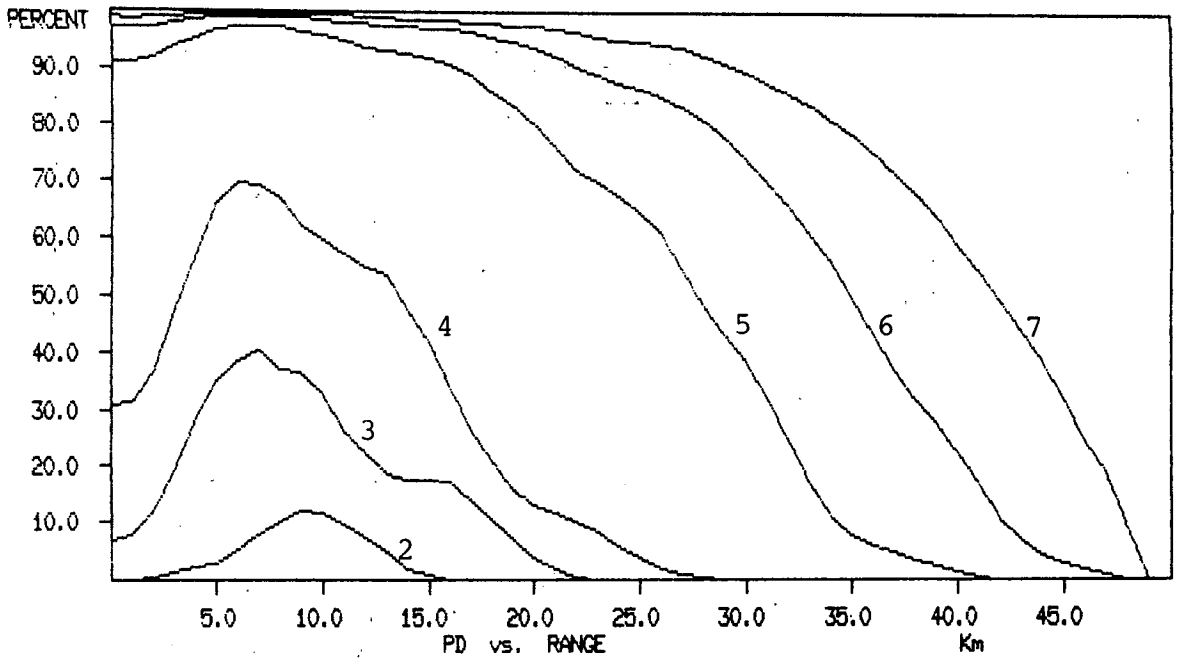

Antenna Height		75 m
Significant Wave Height		0.5 m
Pulse Length		1.0 μsec

Curve 1	Iceberg	1 m x 1 m x 1 m, No Detection
Curve 2	Iceberg	2 m x 5 m x 5 m
Curve 3	Iceberg	4 m x 10 m x 10 m
Curve 4	Iceberg	7 m x 15 m x 15 m
Curve 5	Iceberg	25 m x 60 m x 60 m
Curve 6	Iceberg	45 m x 110 m x 110 m
Curve 7	Iceberg	75 m x 170 m x 170 m

Fig. A-3. Probability of detection for an X-Band radar.

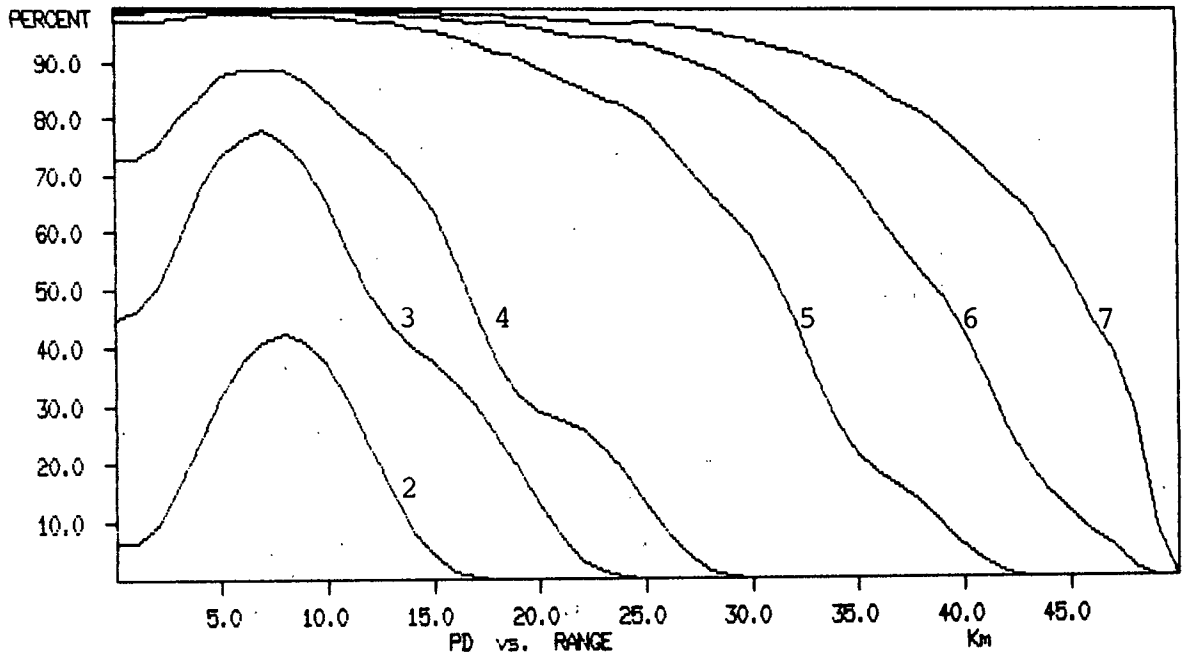

Antenna Height		75 m
Significant Wave Height		0.5 m
Pulse Length		0.25 μsec
Curve 1	Iceberg	1 m x 1 m x 1 m, No Detection
Curve 2	Iceberg	2 m x 5 m x 5 m
Curve 3	Iceberg	4 m x 10 m x 10 m
Curve 4	Iceberg	7 m x 15 m x 15 m
Curve 5	Iceberg	25 m x 60 m x 60 m
Curve 6	Iceberg	45 m x 110 m x 110 m
Curve 7	Iceberg	75 m x 170 m x 170 m

Fig. A-4. Probability of detection for an X-Band radar.

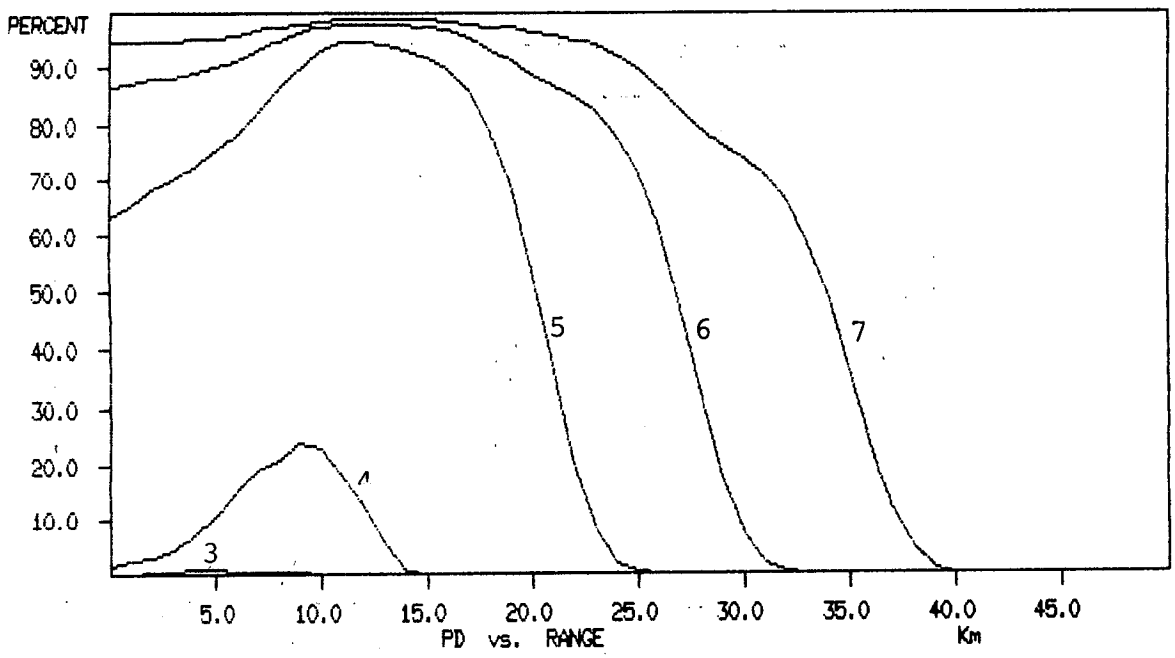

Antenna Height	15 m
Significant Wave Height	2.5 m
Pulse Length	1.0 μsec

Curve 1	Iceberg	1 m x 1 m x 1 m, No Detection
Curve 2	Iceberg	2 m x 5 m x 5 m, No Detection
Curve 3	Iceberg	4 m x 10 m x 10 m
Curve 4	Iceberg	7 m x 15 m x 15 m
Curve 5	Iceberg	25 m x 60 m x 60 m
Curve 6	Iceberg	45 m x 110 m x 110 m
Curve 7	Iceberg	75 m x 170 m x 170 m

Fig. A-5. Probability of detection for an X-Band radar.

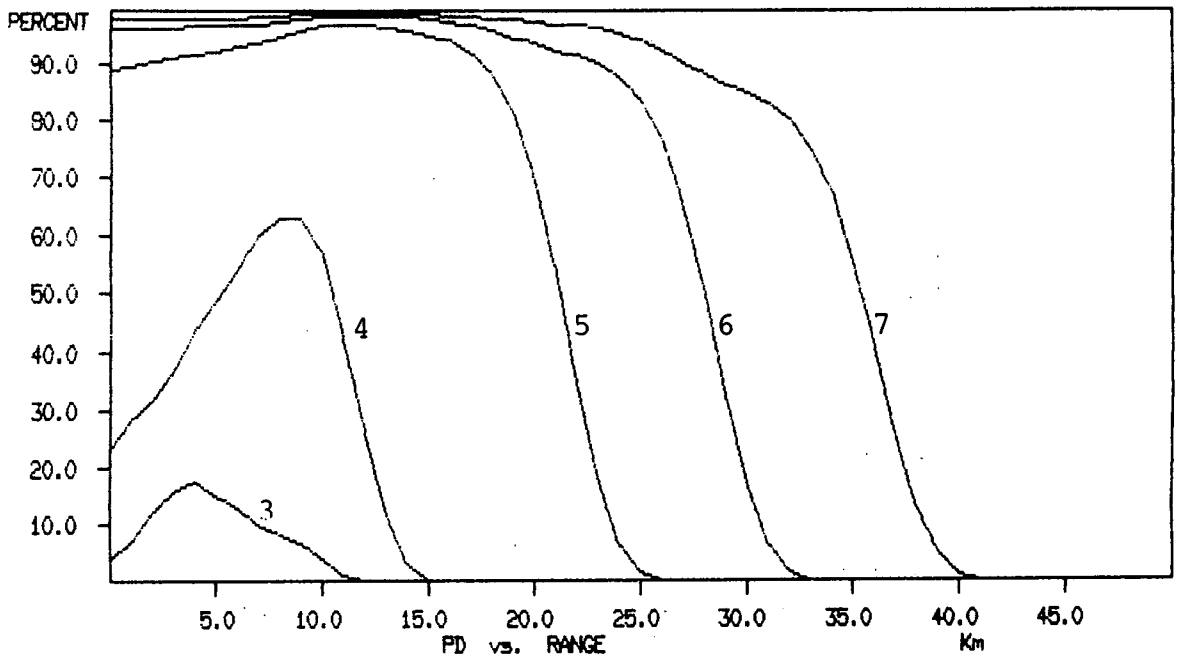

Antenna Height	15 m
Significant Wave Height	2.5 m
Pulse Length	0.25 μsec

Curve 1	Iceberg	1 m x 1 m x 1 m, No Detection
Curve 2	Iceberg	2 m x 5 m x 5 m, No Detection
Curve 3	Iceberg	4 m x 10 m x 10 m
Curve 4	Iceberg	7 m x 15 m x 15 m
Curve 5	Iceberg	25 m x 60 m x 60 m
Curve 6	Iceberg	45 m x 110 m x 110 m
Curve 7	Iceberg	75 m x 170 m x 170 m

Fig. A-6. Probability of detection for an X-Band radar.

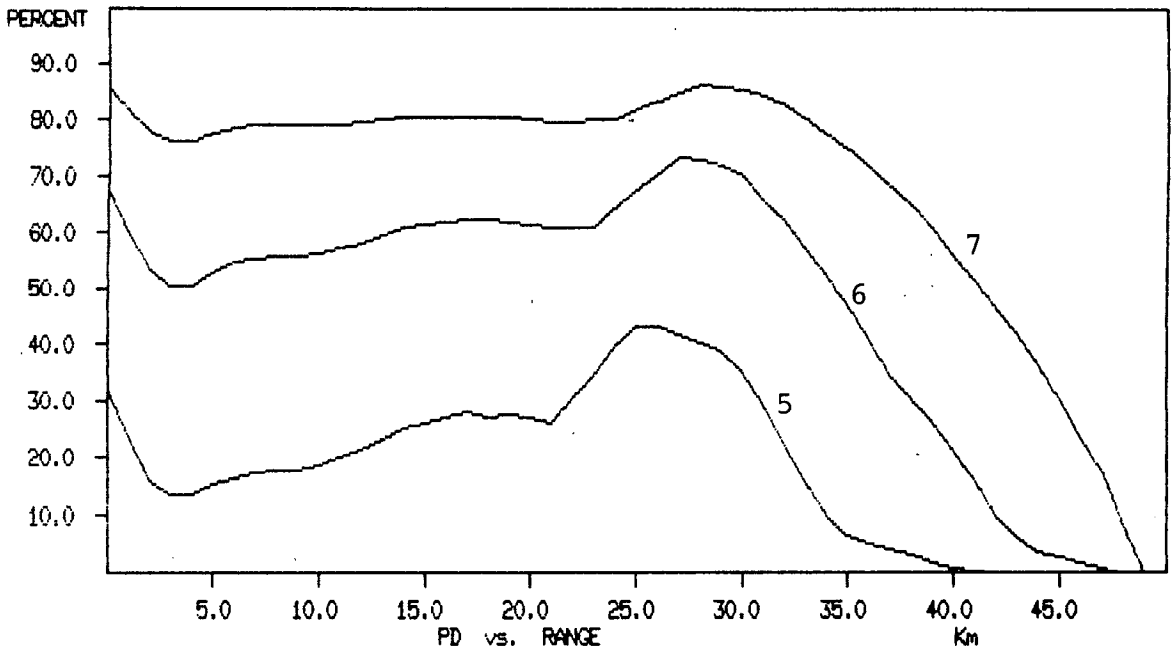

Antenna Height		75 m
Significant Wave Height		2.5 m
Pulse Length		1.0 μsec
Curve 1	Iceberg	1 m x 1 m x 1 m, No Detection
Curve 2	Iceberg	2 m x 5 m x 5 m, No Detection
Curve 3	Iceberg	4 m x 10 m x 10 m, No Detection
Curve 4	Iceberg	7 m x 15 m x 15 m, No Detection
Curve 5	Iceberg	25 m x 60 m x 60 m
Curve 6	Iceberg	45 m x 110 m x 110 m
Curve 7	Iceberg	75 m x 170 m x 170 m

Fig. A-7. Probability of detection for an X-Band radar.

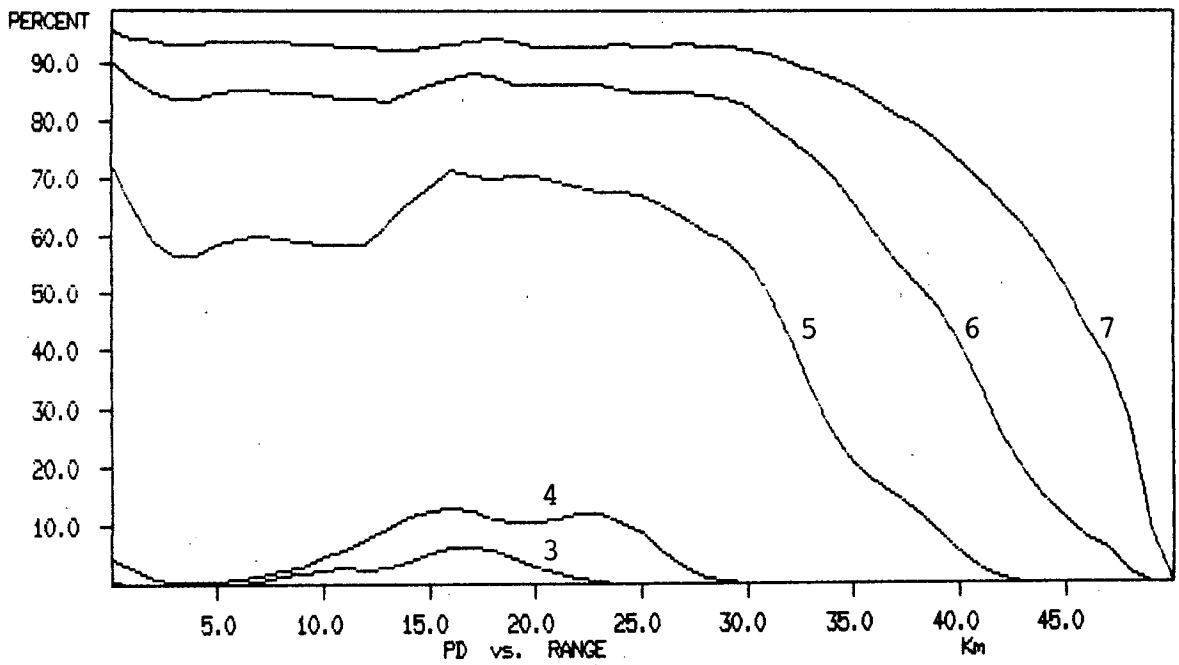

Antenna Height	75 m
Significant Wave Height	2.5 m
Pulse Length	0.25 μsec

Curve 1	Iceberg	1 m x 1 m x 1 m, No Detection
Curve 2	Iceberg	2 m x 5 m x 5 m, No Detection
Curve 3	Iceberg	4 m x 10 m x 10 m
Curve 4	Iceberg	7 m x 15 m x 15 m
Curve 5	Iceberg	25 m x 60 m x 60 m
Curve 6	Iceberg	45 m x 110 m x 110 m
Curve 7	Iceberg	75 m x 170 m x 170 m

Fig. A-8. Probability of detection for an X-Band radar.

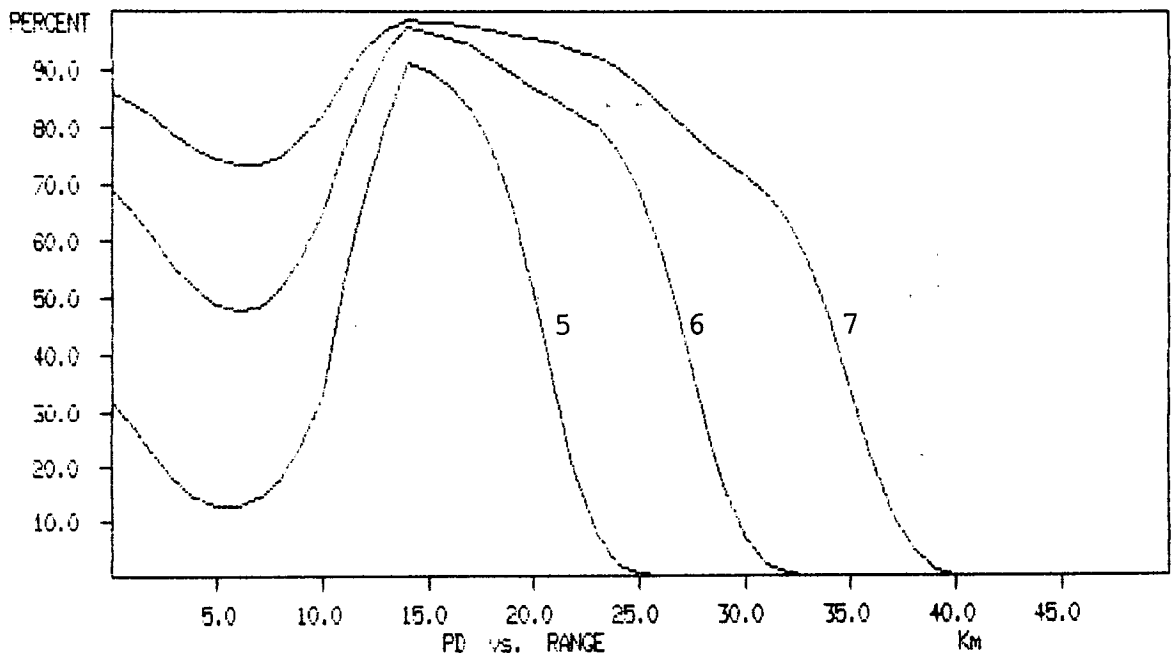

Antenna Height		15 m
Significant Wave Height		5.0 m
Pulse Length		1.0 μsec

Curve 1	Iceberg	1 m x 1 m x 1 m, No Detection
Curve 2	Iceberg	2 m x 5 m x 5 m, No Detection
Curve 3	Iceberg	4 m x 10 m x 10 m, No Detection
Curve 4	Iceberg	7 m x 15 m x 15 m, No Detection
Curve 5	Iceberg	25 m x 60 m x 60 m
Curve 6	Iceberg	45 m x 110 m x 110 m
Curve 7	Iceberg	75 m x 170 m x 170 m

Fig. A-9. Probability of detection for an X-Band radar.

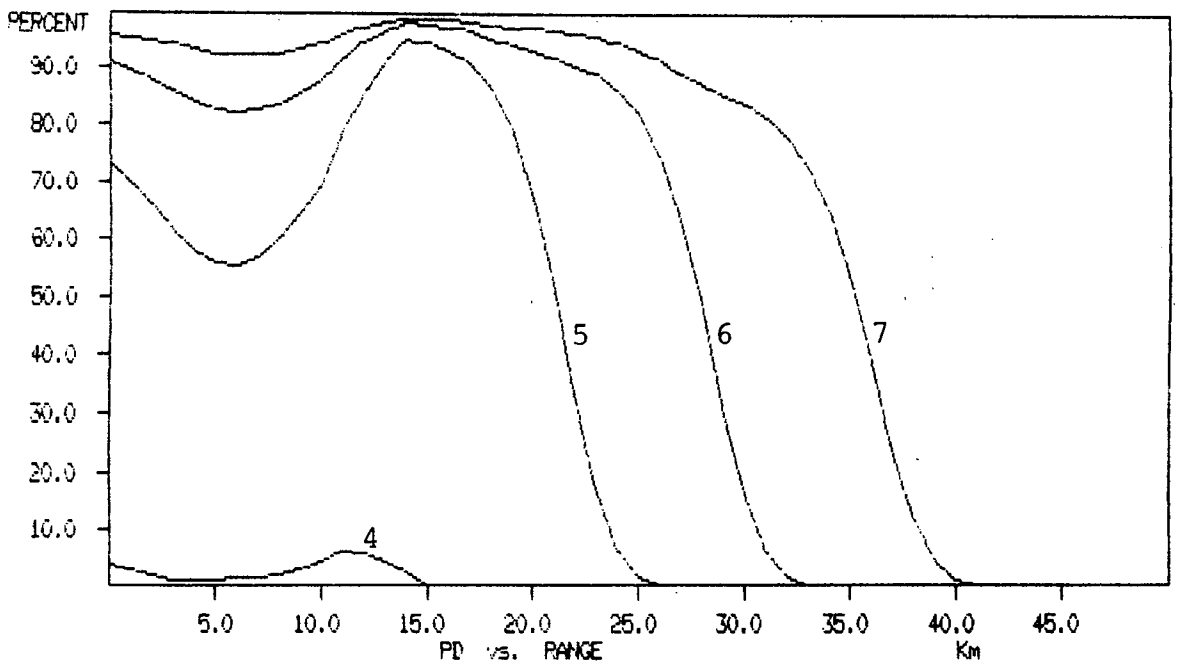

Antenna Height		15 m
Significant Wave Height		5.0 m
Pulse Length		0.25 μsec

Curve 1	Iceberg	1 m x 1 m x 1 m, No Detection
Curve 2	Iceberg	2 m x 5 m x 5 m, No Detection
Curve 3	Iceberg	4 m x 10 m x 10 m, No Detection
Curve 4	Iceberg	7 m x 15 m x 15 m
Curve 5	Iceberg	25 m x 60 m x 60 m
Curve 6	Iceberg	45 m x 110 m x 110 m
Curve 7	Iceberg	75 m x 170 m x 170 m

Fig. A-10. Probability of detection for an X-Band radar.

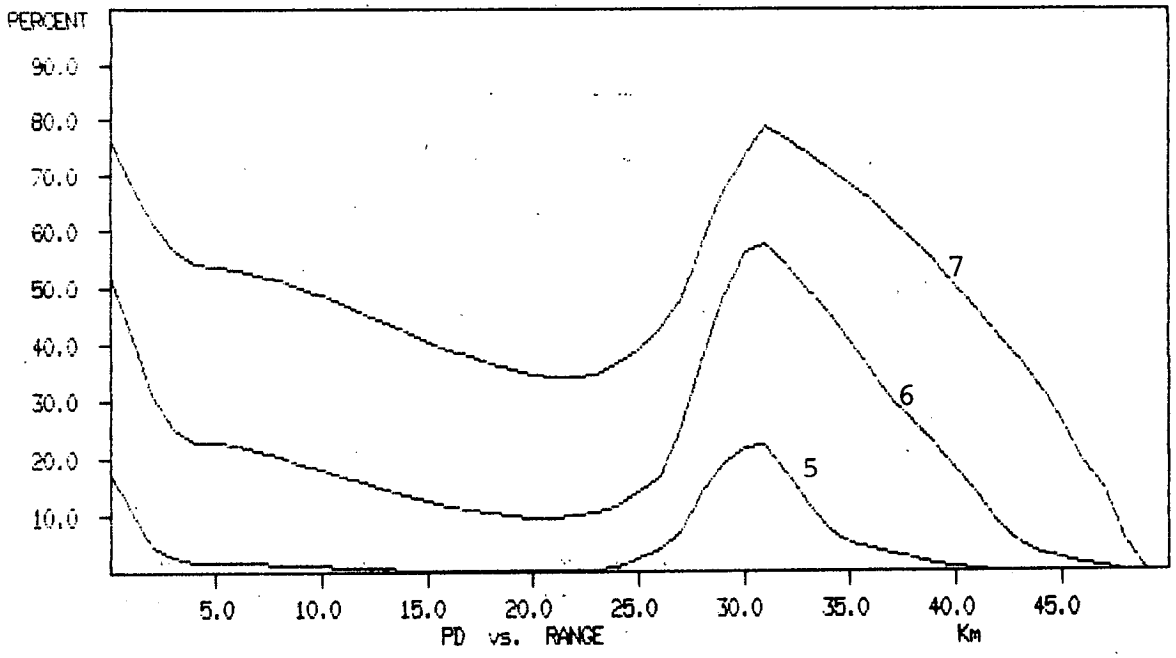

Antenna Height		75 m
Significant Wave Height		5.0 m
Pulse Length		1.0 μsec

Curve 1	Iceberg	1 m x 1 m x 1 m, No Detection
Curve 2	Iceberg	2 m x 5 m x 5 m, No Detection
Curve 3	Iceberg	4 m x 10 m x 10 m, No Detection
Curve 4	Iceberg	7 m x 15 m x 15 m, No Detection
Curve 5	Iceberg	25 m x 60 m x 60 m
Curve 6	Iceberg	45 m x 110 m x 110 m
Curve 7	Iceberg	75 m x 170 m x 170 m

Fig. A-11. Probability of detection for an X-Band radar.

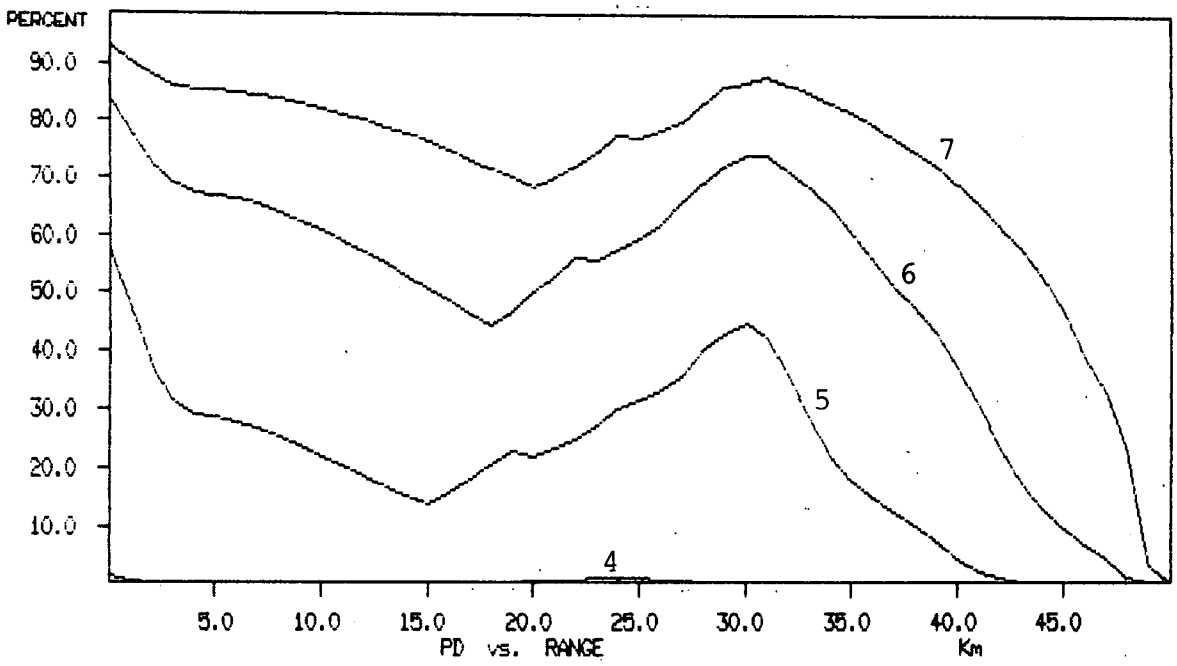

Antenna Height		75 m
Significant Wave Height		5.0 m
Pulse Length		0.25 μsec

Curve 1	Iceberg	1 m x 1 m x 1 m, No Detection
Curve 2	Iceberg	2 m x 5 m x 5 m, No Detection
Curve 3	Iceberg	4 m x 10 m x 10 m, No Detection
Curve 4	Iceberg	7 m x 15 m x 15 m
Curve 5	Iceberg	25 m x 60 m x 60 m
Curve 6	Iceberg	45 m x 110 m x 110 m
Curve 7	Iceberg	75 m x 170 m x 170 m

Fig. A-12. Probability of detection for an X-Band radar.

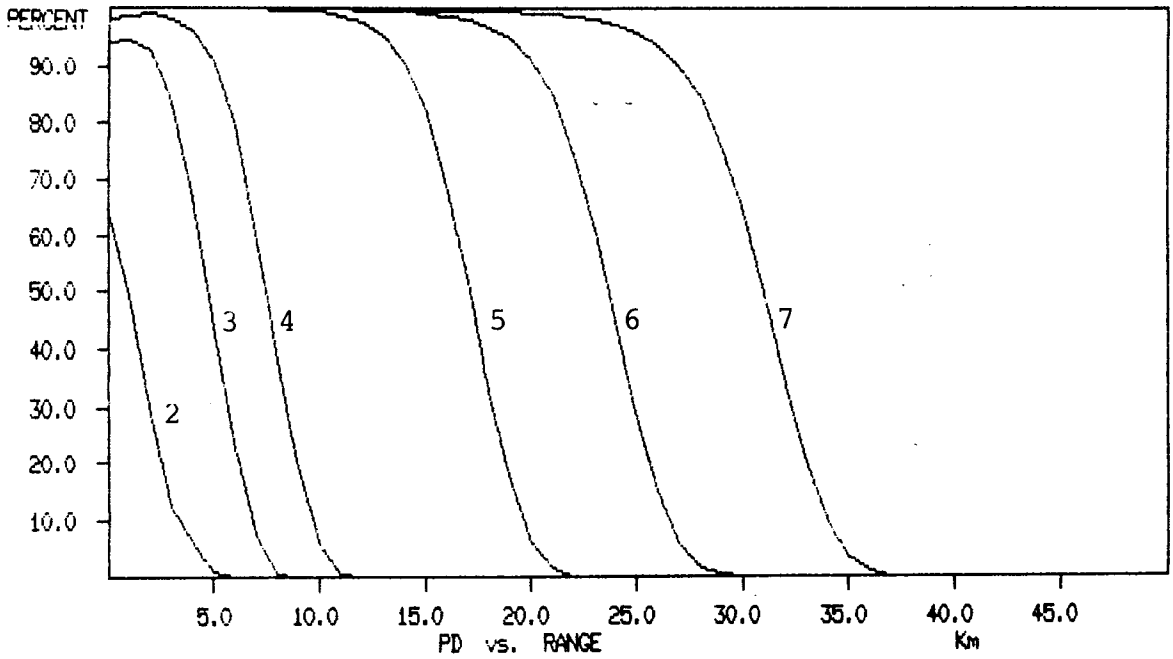

Antenna Height	15 m
Significant Wave Height	0.5 m
Pulse Length	1.0 μsec

Curve 1	Iceberg	1 m x 1 m x 1 m, No Detection
Curve 2	Iceberg	2 m x 5 m x 5 m
Curve 3	Iceberg	4 m x 10 m x 10 m
Curve 4	Iceberg	7 m x 15 m x 15 m
Curve 5	Iceberg	25 m x 60 m x 60 m
Curve 6	Iceberg	45 m x 110 m x 110 m
Curve 7	Iceberg	75 m x 170 m x 170 m

Fig. A-13. Probability of detection for an S-Band radar.

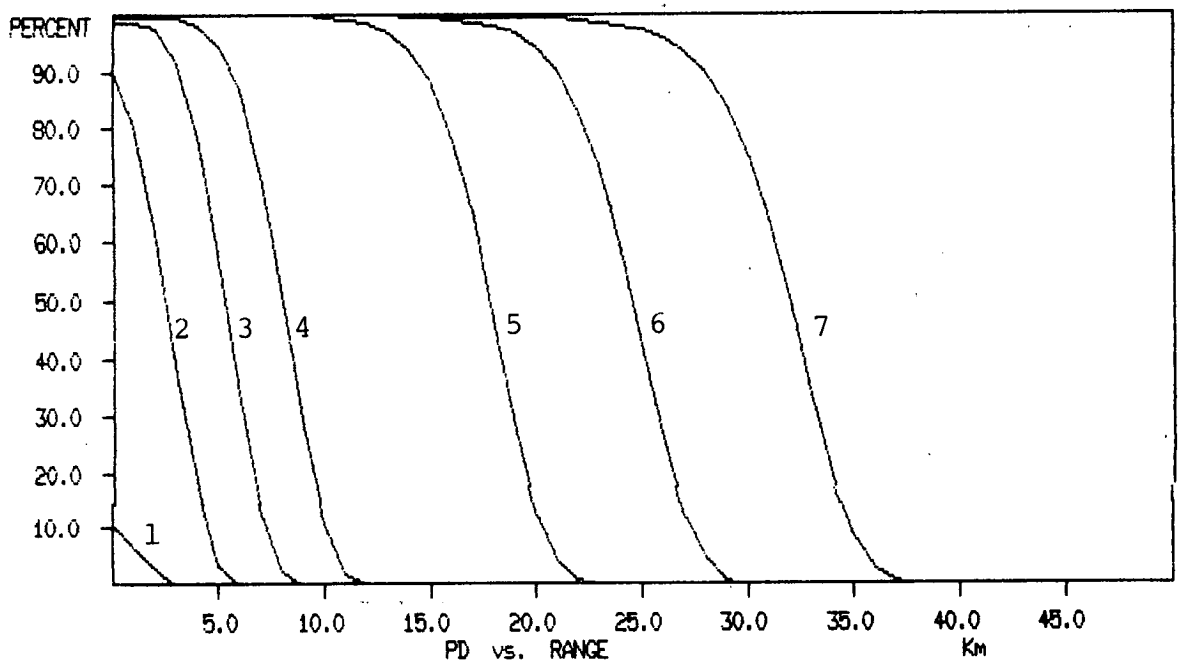

Antenna Height		15 m
Significant Wave Height		0.5 m
Pulse Length		0.25 μsec

Curve 1	Iceberg	1 m x 1 m x 1 m
Curve 2	Iceberg	2 m x 5 m x 5 m
Curve 3	Iceberg	4 m x 10 m x 10 m
Curve 4	Iceberg	7 m x 15 m x 15 m
Curve 5	Iceberg	25 m x 60 m x 60 m
Curve 6	Iceberg	45 m x 110 m x 110 m
Curve 7	Iceberg	75 m x 170 m x 170 m

Fig. A-14. Probability of detection for an S-Band radar.

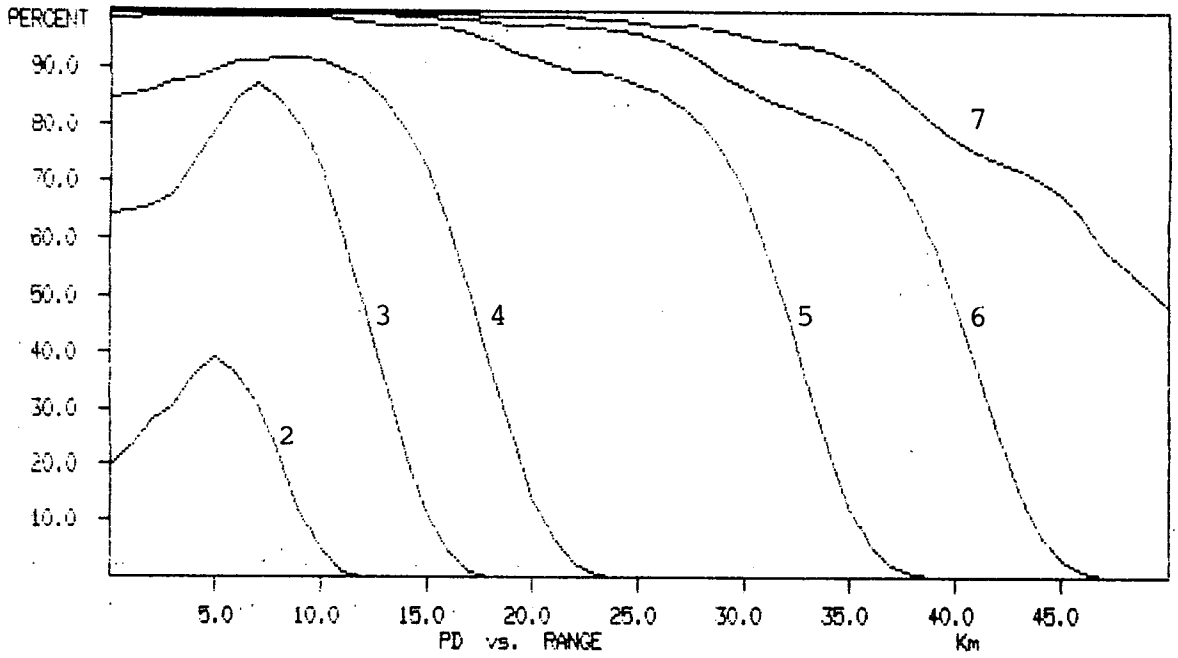

Antenna Height	75 m
Significant Wave Height	0.5 m
Pulse Length	1.0 μsec

Curve 1	Iceberg	1 m x 1 m x 1 m, No Detection
Curve 2	Iceberg	2 m x 5 m x 5 m
Curve 3	Iceberg	4 m x 10 m x 10 m
Curve 4	Iceberg	7 m x 15 m x 15 m
Curve 5	Iceberg	25 m x 60 m x 60 m
Curve 6	Iceberg	45 m x 110 m x 110 m
Curve 7	Iceberg	75 m x 170 m x 170 m

Fig. A-15. Probability of detection for an S-Band radar.

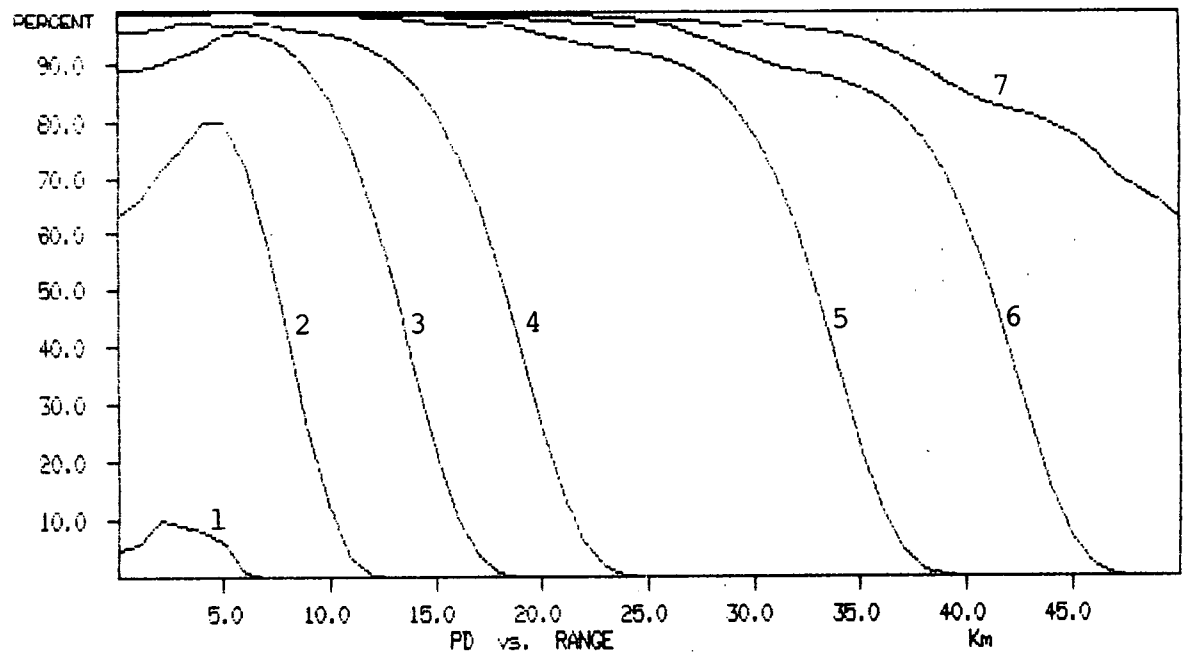

Antenna Height	75 m
Significant Wave Height	0.5 m
Pulse Length	0.25 μsec

Curve 1	Iceberg	1 m x 1 m x 1 m
Curve 2	Iceberg	2 m x 5 m x 5 m
Curve 3	Iceberg	4 m x 10 m x 10 m
Curve 4	Iceberg	7 m x 15 m x 15 m
Curve 5	Iceberg	25 m x 60 m x 60 m
Curve 6	Iceberg	45 m x 110 m x 110 m
Curve 7	Iceberg	75 m x 170 m x 170 m

Fig. A-16. Probability of detection for an S-Band radar.

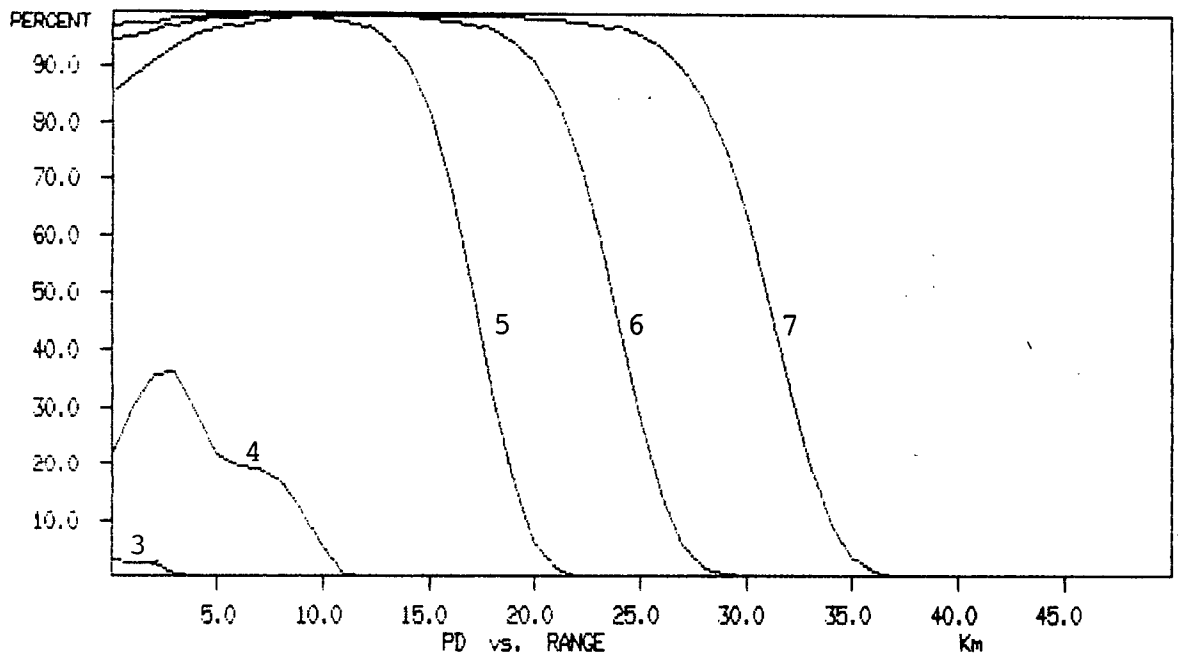

Antenna Height		15 m
Significant Wave Height		2.5 m
Pulse Length		1.0 μsec

Curve 1	Iceberg	1 m x 1 m x 1 m, No Detection
Curve 2	Iceberg	2 m x 5 m x 5 m, No Detection
Curve 3	Iceberg	4 m x 10 m x 10 m
Curve 4	Iceberg	7 m x 15 m x 15 m
Curve 5	Iceberg	25 m x 60 m x 60 m
Curve 6	Iceberg	45 m x 110 m x 110 m
Curve 7	Iceberg	75 m x 170 m x 170 m

Fig. A-17. Probability of detection for an S-Band radar.

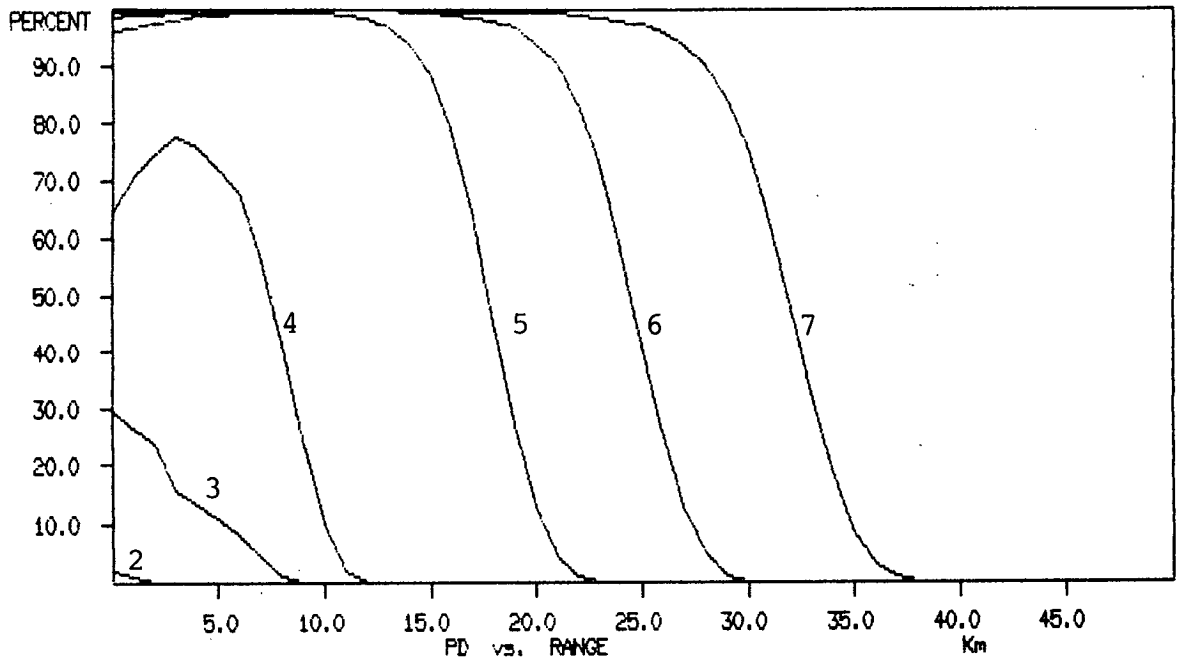

Antenna Height	15 m
Significant Wave Height	2.5 m
Pulse Length	0.25 μsec

Curve 1	Iceberg	1 m x 1 m x 1 m, No Detection
Curve 2	Iceberg	2 m x 5 m x 5 m
Curve 3	Iceberg	4 m x 10 m x 10 m
Curve 4	Iceberg	7 m x 15 m x 15 m
Curve 5	Iceberg	25 m x 60 m x 60 m
Curve 6	Iceberg	45 m x 110 m x 110 m
Curve 7	Iceberg	75 m x 170 m x 170 m

Fig. A-18. Probability of detection for an S-Band radar.

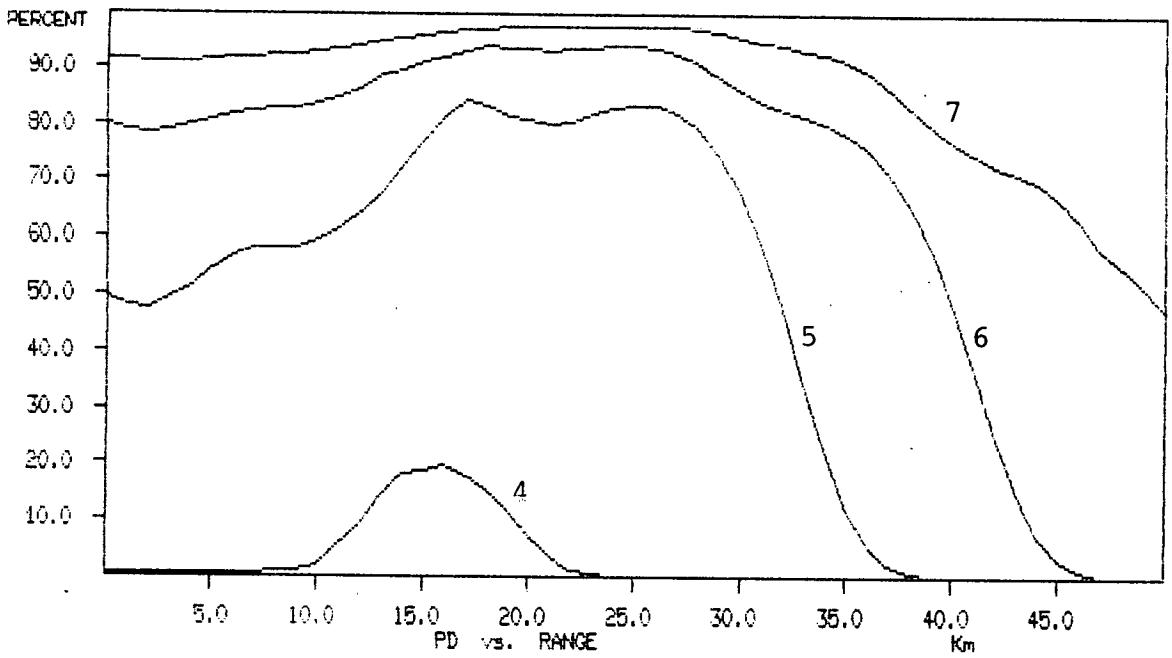

Antenna Height	75 m
Significant Wave Height	2.5 m
Pulse Length	1.0 μsec

Curve 1	Iceberg	1 m x 1 m x 1 m, No Detection
Curve 2	Iceberg	2 m x 5 m x 5 m, No Detection
Curve 3	Iceberg	4 m x 10 m x 10 m, No Detection
Curve 4	Iceberg	7 m x 15 m x 15 m
Curve 5	Iceberg	25 m x 60 m x 60 m
Curve 6	Iceberg	45 m x 110 m x 110 m
Curve 7	Iceberg	75 m x 170 m x 170 m

Fig. A-19. Probability of detection for an S-Band radar.

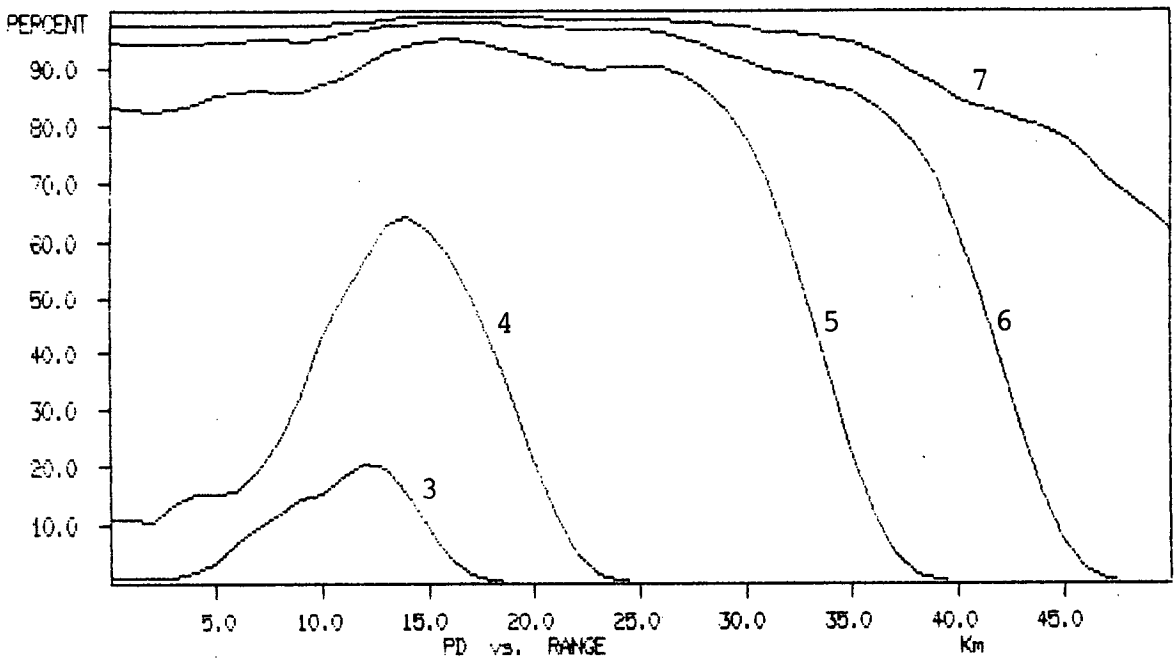

Antenna Height	75 m
Significant Wave Height	2.5 m
Pulse Length	0.25 μsec

Curve 1	Iceberg	1 m x 1 m x 1 m, No Detection
Curve 2	Iceberg	2 m x 5 m x 5 m, No Detection
Curve 3	Iceberg	4 m x 10 m x 10 m
Curve 4	Iceberg	7 m x 15 m x 15 m
Curve 5	Iceberg	25 m x 60 m x 60 m
Curve 6	Iceberg	45 m x 110 m x 110 m
Curve 7	Iceberg	75 m x 170 m x 170 m

Fig. A-20. Probability of detection for an S-Band radar.

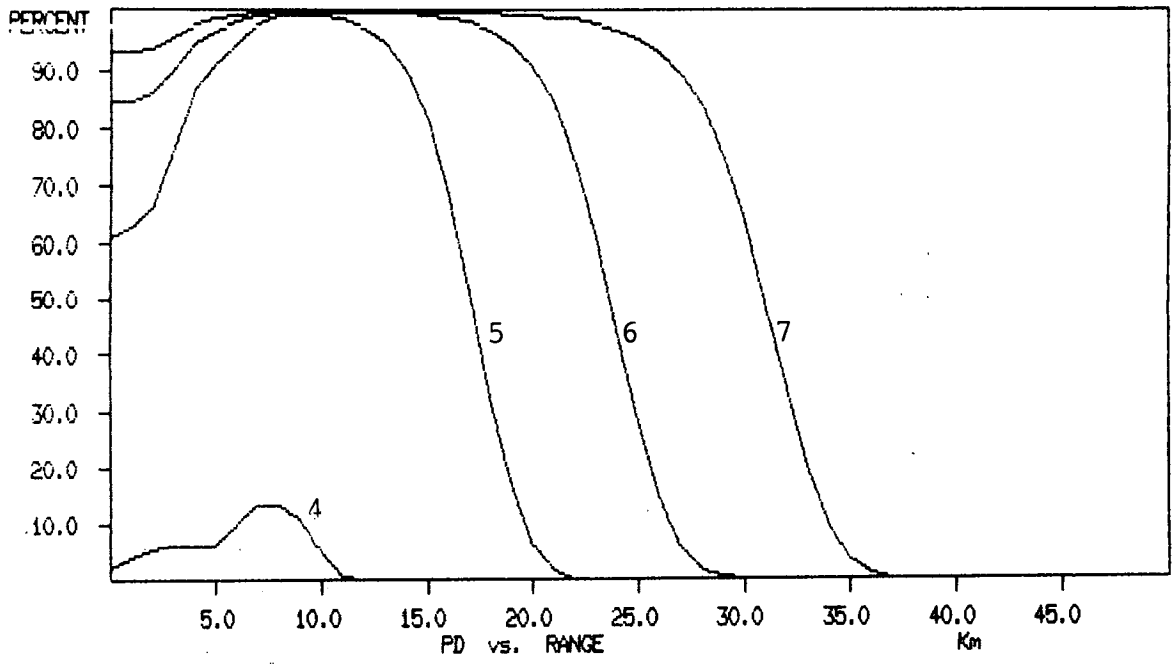

Antenna Height	15 m
Significant Wave Height	5.0 m
Pulse Length	1.0 μsec

Curve 1	Iceberg	1 m x 1 m x 1 m, No Detection
Curve 2	Iceberg	2 m x 5 m x 5 m, No Detection
Curve 3	Iceberg	4 m x 10 m x 10 m, No Detection
Curve 4	Iceberg	7 m x 15 m x 15 m
Curve 5	Iceberg	25 m x 60 m x 60 m
Curve 6	Iceberg	45 m x 110 m x 110 m
Curve 7	Iceberg	75 m x 170 m x 170 m

Fig. A-21. Probability of detection for an S-Band radar.

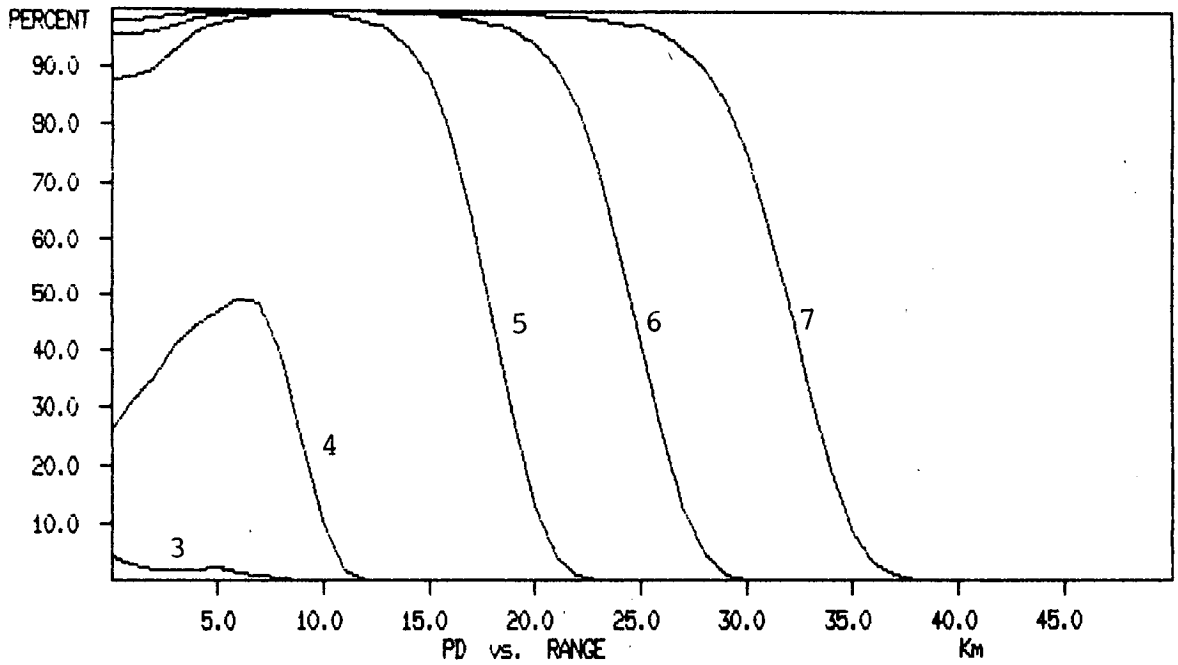

Antenna Height	15 m
Significant Wave Height	5.0 m
Pulse Length	0.25 μsec

Curve 1	Iceberg	1 m x 1 m x 1 m, No Detection
Curve 2	Iceberg	2 m x 5 m x 5 m, No Detection
Curve 3	Iceberg	4 m x 10 m x 10 m
Curve 4	Iceberg	7 m x 15 m x 15 m
Curve 5	Iceberg	25 m x 60 m x 60 m
Curve 6	Iceberg	45 m x 110 m x 110 m
Curve 7	Iceberg	75 m x 170 m x 170 m

Fig. A-22. Probability of detection for an S-Band radar.

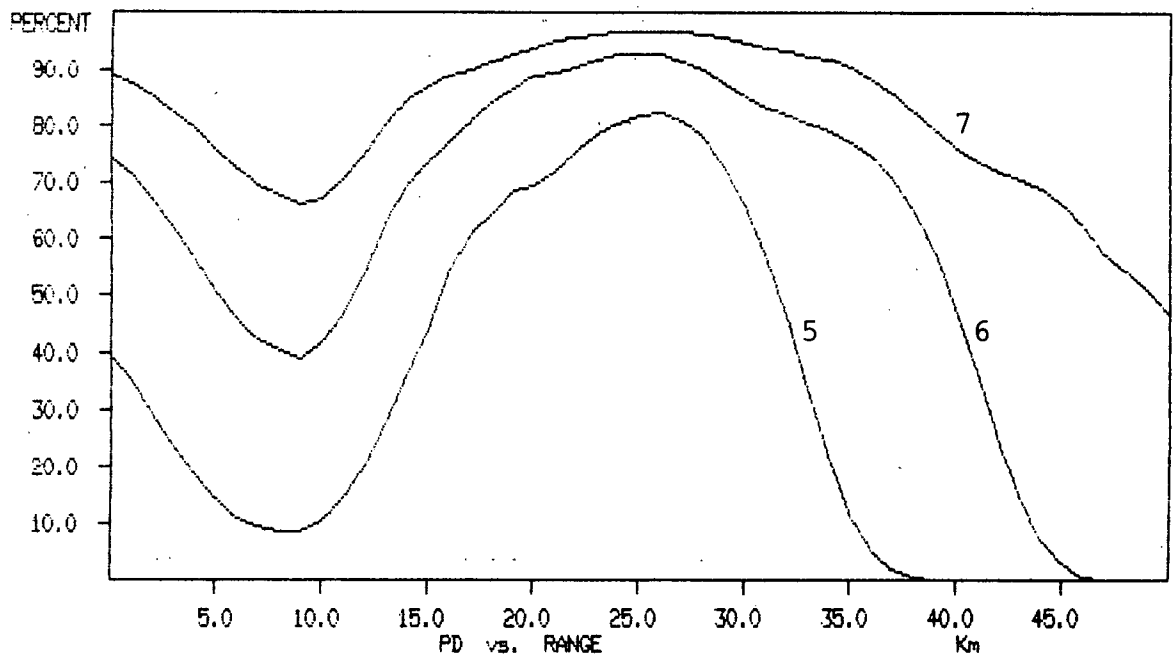

Antenna Height		75 m
Significant Wave Height		5.0 m
Pulse Length		1.0 μsec

Curve 1	Iceberg	1 m x 1 m x 1 m, No Detection
Curve 2	Iceberg	2 m x 5 m x 5 m, No Detection
Curve 3	Iceberg	4 m x 10 m x 10 m, No Detection
Curve 4	Iceberg	7 m x 15 m x 15 m, No Detection
Curve 5	Iceberg	25 m x 60 m x 60 m
Curve 6	Iceberg	45 m x 110 m x 110 m
Curve 7	Iceberg	75 m x 170 m x 170 m

Fig. A-23. Probability of detection for an S-Band radar.

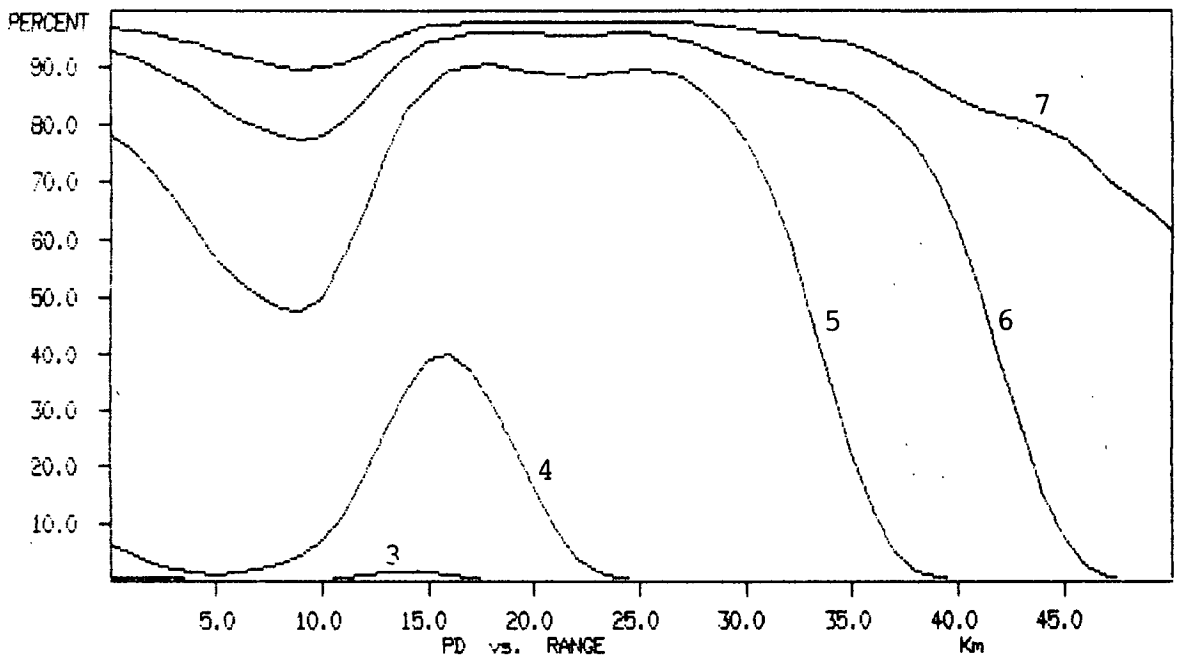

Antenna Height		75 m
Significant Wave Height		5.0 m
Pulse Length		0.25 μsec
Curve 1	Iceberg	1 m x 1 m x 1 m, No Detection
Curve 2	Iceberg	2 m x 5 m x 5 m, No Detection
Curve 3	Iceberg	4 m x 10 m x 10 m
Curve 4	Iceberg	7 m x 15 m x 15 m
Curve 5	Iceberg	25 m x 60 m x 60 m
Curve 6	Iceberg	45 m x 110 m x 110 m
Curve 7	Iceberg	75 m x 170 m x 170 m

Fig. A-24. Probability of detection for an S-Band radar.

Appendix 3

Specifications

The following specifications are extracted from manufacturers brochures. Company information is given after the specifications.

RADAR REFLECTORS

The most effective radar reflectors for balloon tracking purposes are of the corner type. Such reflectors must be large enough to be followed at long range, light in construction and capable of being folded for storage and transit.

The corner reflectors have reflecting planes of metallised nylon mesh assembled on aluminium alloy tube frames. When erected they are braced by steel wires to maintain the correct geometry. The mesh is proofed after metallisation with a special protective coating which improves the resistance of the mesh to abrasion and renders it highly resistant to oil, water and environmental conditions.

Typical Specifications (Metallised Mesh)

Size of reflecting panels		Weight	Radar cross section of each corner		
Right Side	Hyp.		9 GHz I Band	6 GHz G/H Band	3 GHz E/F Band
mm	mm	grams	m^2	m^2	m^2
480	680	248	120	45	10
650	920	320	420	150	35
970	1370	513	2060	740	190

Typical Specifications (Aluminum Coated Mylar)

Type Number	Tetrahedral TD75
Size of reflecting panels:	
Right side	530 mm
Hypotenuse	750 mm
Weight	100 grams
Radar cross section of each corner:	
9 GHz I Band	180 m2
6 GHz G/H Band	65 m2
3 GHz E/F Band	15 m2

Expanding Balloon Covers

For radar wind finding at medium ranges and altitudes, Expanding Balloon Covers offer a lighter alternative to the radar corner reflector. An Expanding Balloon Cover consists of a radar-reflective nylon mesh which is slipped over an 80 - 100 gram balloon during inflation.

Spherical Balloon Covers

For calibrating and checking the performance of radar equipment, a standard target is necessary which must have a known echoing area.

Spherical Balloon Covers are supplied in diameters of 0.61 m, 1.00 m and 1.22 m. These sizes are suitable for use with 50, 80 or 100 gram balloons.

Radar Reflective and Screening Meshes

High quality nylon is metallised under strictly controlled conditions to achieve the design characteristics. The mesh is designed to be responsive to radar systems using 6 and 9 GHz (GH and I Bands). The hexagonal mesh for 6 and 9 GHz has a hole spacing of 8 per centimetre. These spacings give a reflection efficiency of at least 95% at their respective wavelengths.

Chaff

The Chaff is made from aluminium coated glass filament of a nominal 25 microns diameter (0.001 inch) and cut to give a radar response typically over the frequencies 5 to 22 Gigahertz. This can be varied easily to suit a user's particular requirement, e.g. for training at a particular frequency.

Chemring PLC
Alchem Works
Fratton Trading Estate
Portsmouth P04 8SX
England
Telephone: Portsmouth (0705) 735457
Telex: 86242

X-BAND RADAR TRANSPONDER

Specifications

General Characteristics:

Frequency range	8800 to 9500 MHz (tunable)
Primary power	24 to 30 VDC (floating ground)
Primary current (typical)	0.55 amp. standby; 0.7 amp. at 1000 pps
Recovery time	50 μ sec max. for input signal levels differing by up to 65 dB
Transponder delay:	
Standard	1 μ sec; settable 1.0 to 4.3 μ sec
Variation with signal level.	0.05 μ sec max. from -62 dBm to 0 dBm
Pulse delay jitter	0.02 μ sec max. for signals greater than -55 dBm
Dimensions	3.36 x 2.90 x 3.96 inches (8.53 x 7.37 x 10.06 cm)
Volume	37.8 cu. in. (619.54 cu. cm)
Weight	3.3 pounds (1.5 kg)

Receiver Characteristics:

Off-frequency rejection	60 dB image; 80 dBm min., 0.15 to 10,000 MHz
Sensitivity (99% reply)	-68 dBm
Interrogation code	Single pulse
Pulse width	0.25 to 5.0 μ sec (single-pulse)
Signal input (maximum)	+20 dBm
Bandwidth	18 MHz

Transmitter Characteristics:

Power output (peak)	400 watts, typical 300 watts, minimum
Duty cycle	0.002 maximum
Output pulse width	0.3 $\pm$ 0.1 μ sec or 0.5 $\pm$ 0.1 μ sec
Pulse rise time (10% to 90%)	0.1 μsec, maximum
Pulse fall time (90% to 10%)	0.2 μ sec, maximum

Motorola Corporation
Government Electronics Division
8201 East McDowell Road
Scottsdale, Arizona
85252

RADIO DIRECTION FINDER

The AN/SRD-501 equipment will detect and determine the direction of any signal of known frequency. It is a dual channel, manually tuned, superheterodyne receiver.

Frequency	-	.060 MHz to 30 MHz in 6 ranges.
Modulation	-	Receives AM, MCW, SSB, CW, FM, FSK, and PPM signals.
Frequency Calibration	-	Harmonics of internal crystal controlled .1 MHz Oscillator. Calibration of tuning dial controlled by front panel frequency correction control.
Display	-	DF - relative bearing on 5" CRT with cursor, accuracy is $\pm$ 2°.
Monitor	-	Audio output of receiver, with BFO and modulation selection available.
Antenna	-	Crossed loops (DF), Vertical dipole (sense), Polarization vertical.
Range	-	System provide reliable bearing information within 60 to 80 miles of transmitter with best reception below 4 MHz because of sky wave effects at higher frquencies.
Calibration	-	It is necessary to carry out calibration at different frequencies with calibration charts due to superstructure effect on radiation patterns.

LORAN RETRANSMISSION

Presently marketed as a Vehicle Tracking System (VTS) by Canadian Marconi for II Morrow Corporation, the II Morrow VTS is a Loran C based system which enables you to monitor the location and movement of a fleet of vehicles from a dispatch, command or control center.

The VTS system is built around a II Morrow receiver which picks up locating signals from Loran C. The receiver is mounted in each vehicle and may be tied into the existing radio transceiver.

A polling transmitter at central control polls each vehicle in turn. When the transceiver in the vehicle receives its code, it is activated, thereby transmitting the vehicle's location to the central control.

The control console receives the digital signal, processes it and feeds it into a high resolution color TV monitor on which a map of the area is shown for visual display.

Each vehicle appears on the map as a rectangle with the vehicle's alphanumeric code inside. Each system can currently track up to 256 vehicles.

II Morrow Inc.
P.O. Box 13549
Salem, OR
USA 97309
Telephone: (503) 581-8101
TWX: 510-599-0110

Appendix 4

Radio Transmission Loss at 2 and 4 MHz

TRANSMISSION LOSS

The free space vertical electric field for an elementary dipole source in the horizontal plane is given as;

$$E_0 = \frac{C_d}{4\pi} \frac{\exp(-jk\rho)}{\rho} \tag{1}$$

where

$C_d = -j\ \omega\ \mu_0\ I_0 dl$

$k = \frac{2\pi}{\lambda}$

$= \text{wave number}$

$\rho = \text{distance from source}$

$j = \sqrt{-1}$.

Similarly, the electric field at a distance over a homogeneous spherical earth for the same source, is given as;

$$E_z = \frac{2C_d}{4\pi} \frac{W_r}{\rho} \exp(-jk\rho) \tag{2}$$

where,

$W_r = \text{spherical earth attenuation function}$

From Jasik [1961], the transmitting antenna gain in the horizontal direction is,

$$G_T = \frac{2\pi \left|E_0\right|^2}{\eta_0 P_t} \tag{3}$$

where;

$\eta_0 = \text{intrinsic impedance of free space}$

$P_t = \text{transmitted power}$

The received power for an antenna of effective area A_r is

$$P_R = \frac{\left|E_z\right|^2}{2\eta_0} A_r = \frac{\lambda_0^2 G_R}{4\pi} \frac{\left|E_z\right|^2}{2\eta_0} \tag{4}$$

where

G_R = receive antenna gain

By using equations (1) through (4), the transmission loss may be written as;

$$TL = \frac{P_R}{P_T} = \frac{4\lambda_0^2 G_T G_R \left| W_r \right|^2}{(4\pi)^2 \rho^2} \tag{5}$$

where

TL = transmission loss

The spherical earth attenuation function, W_r, may be estimated using standard expressions as developed by Fock [1965], Bremmer [1949] and Wait [1970]. These expressions are based on the general formulation for the electric field on a sphere as proposed by Watson [1919]. For antennas located close to the earth's surface, the residue series approximation as proposed by Fock is most suitable. This series approximation may be written using the surface impedance concept to facilitate the implementation of the roughness effect. The roughness effect is included in the propagation model by a modification to the surface impedance which accounts for apparent changes in the impedance due to the surface roughness. Several authors, Barrick [1971], Wait [1959] and Srivastava [1984] have derived expressions for such a modified surface impedance for the ocean surface using various techniques. For this study, the expressions as derived by Srivastava using a Neumann-Pierson Wave Height Spectral Density model for wind driven sea have been used.

Figure 1 represents the predicted transmission loss at 2.0 MHz for two typical sea conditions. The transmission loss in dB using wind speed in nautical miles per hour to describe the surface has been plotted versus distance. Typical values for the permittivity ϵ_r $(= 80.0)$ and the

conductivity σ ($= 4.0 mhos/m$) are assumed, as well as non directive transmitting and receiving antennas. The transmitted power has been assumed to be one watt, for convenience. This plot may be used to predict the required transmitted power for a given receiver sensitivity, the required receiver sensitivity for a given transmitted power or the maximum range of a system with specified sensitivity and transmitted power. The limiting effects of any noises (atmospheric, man made, receiver) have been neglected, but in the HF band may be a significant factor in specifying a communications system. Figure 2 represents a similar plot for an operating frequency of 4.0 MHz.

FIGURE 1

2.0 MHz. Transmission Losses

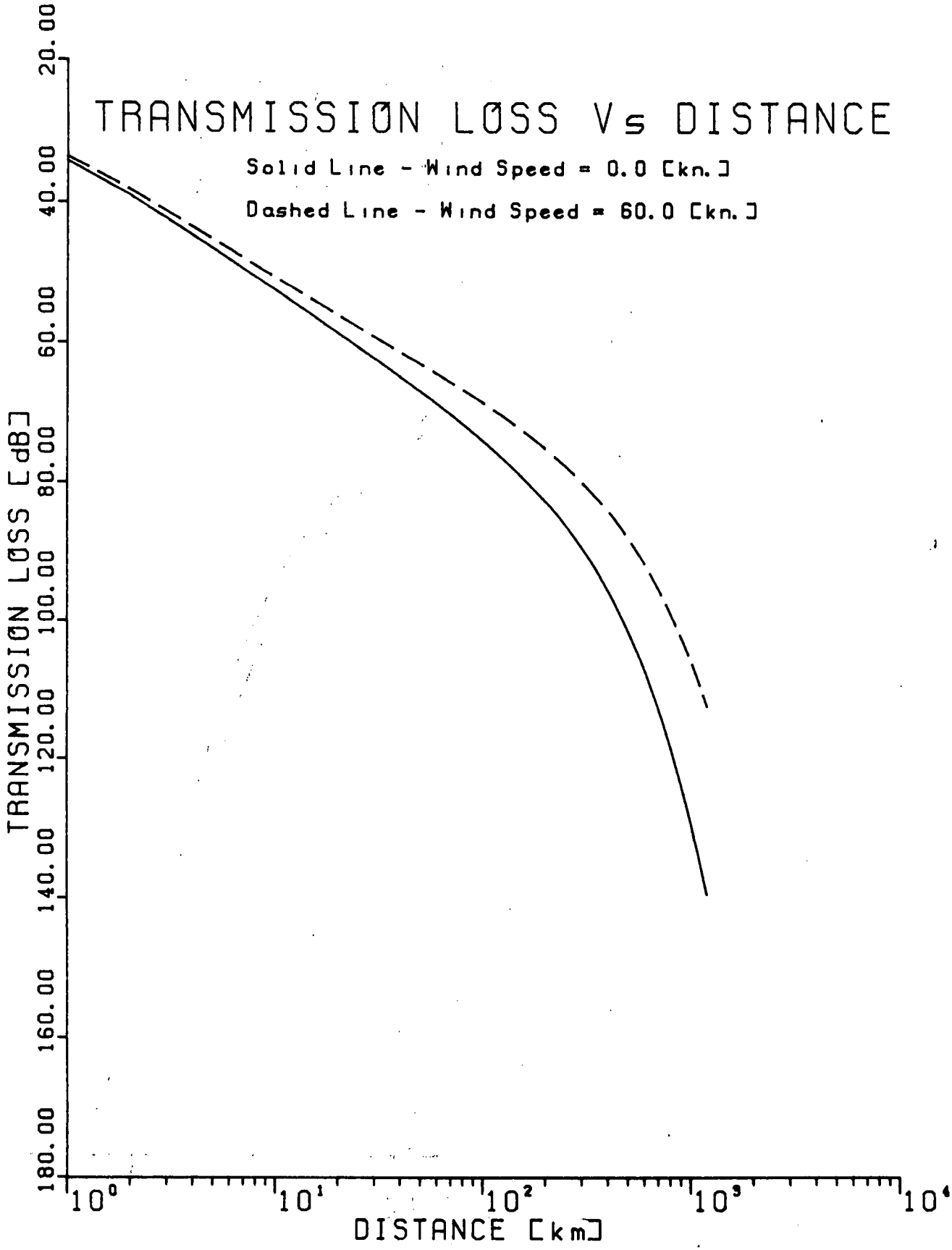

FIGURE 2

4.0 MHz. Transmission Losses

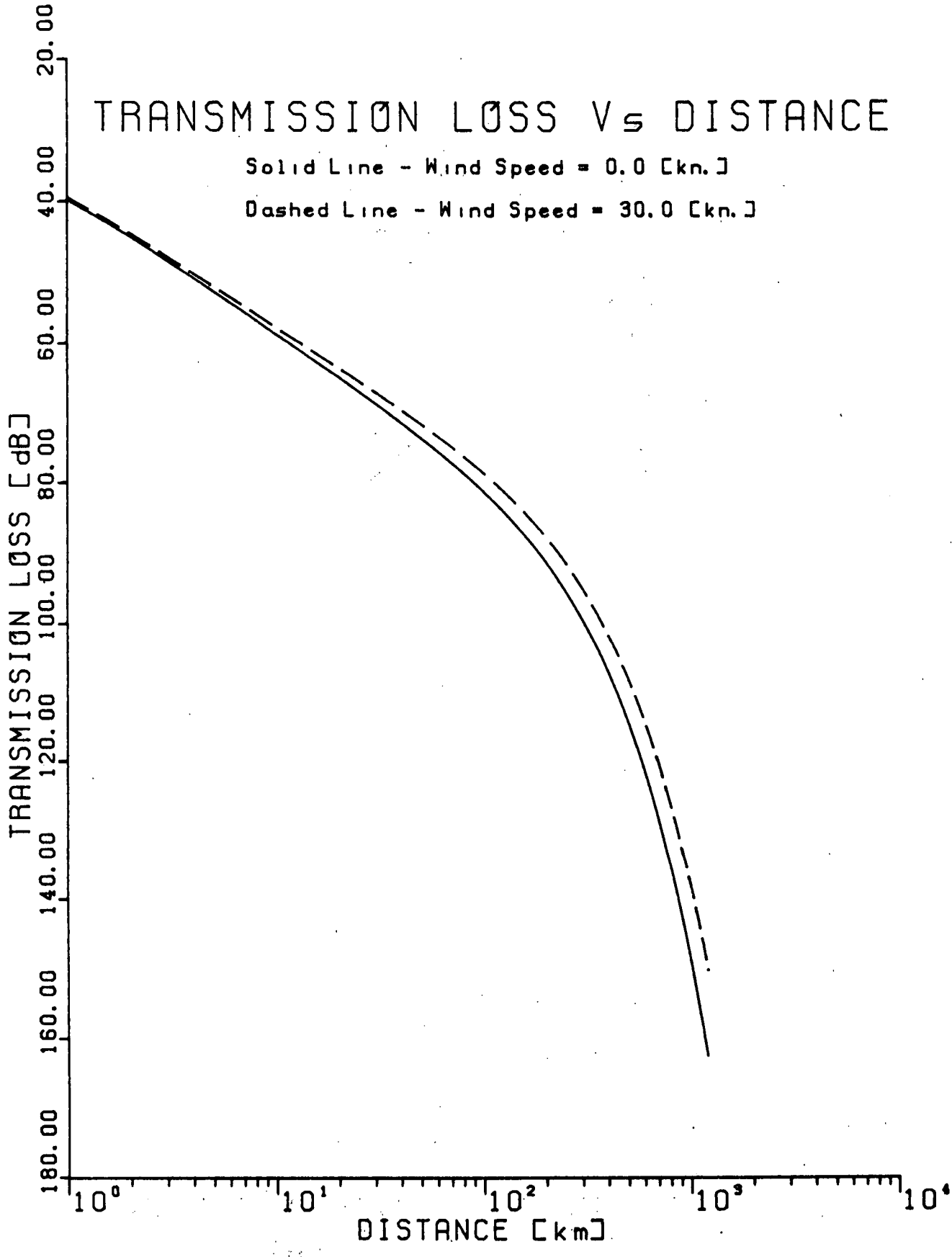

REFERENCES

Allen, J.H. 1971. Cruise report C.S.S. "Dawson" June 2 - June 12, 1971. Faculty of Engineering and Applied Science, Memorial University of Newfoundland.

Barrick, D.E. 1970. Rough surfaces. Vol. II of Radar cross section handbook, edited by George T. Ruck. Plenum Press, New York.

Blake, L.V. 1980. Radar range performance analysis. D.C. Heath and Company.

Budinger, T.F. 1960. Iceberg detection by radar. International Ice Patrol Bulletin No. 45, United States Coast Guard.

Butters, B.C.F. 1982. Chaff. Proceedings of Institute of Electrical and Electronic Engineers 129(F)(3).

Crissman, R.D. and M.W. Evans. 1985. An HF CODAR doppler transponder system. Proceedings of the Conf. Arctic '85/ASCE, San Francisco, CA, March 25-27, 1985.

Dawe, B.R. 1985. A radar cross section model for icebergs. IEEE 1985 International Radar Conference, Arlington, Virgina, May 6-9, 1985.

Diemand, D. 1984. A shoulder-launched projectile for subsurface measurement of iceberg temperatures. Workshop on Ice Penetration Technologies, CRREL Report 84-33, June 12, 1984.

Grant, D.A. 1971. Iceberg tracking off the Labrador coast by aircraft of Maritime Command, 1970-1971. Department of National Defence. Proceedings of the Canadian Seminar on Icebergs, Halifax, Nova Scotia.

Gray, A.L., R.K. Hawkins, C.E. Livingstone, R. Lowry, R. Lawson and R. Rawson. 1979. The influence of incidence angle on microwave radar returns of "targets" in an ocean background. Proceedings of 13th International Symposium on Remote Sensing of the Environment, Ann Arbor, Michigan, April 23-27, 1979, pp 1815-1837.

Greger, M. 1984. Kites. Library of Congress, Catalog No. 84-90384.

Harwood, T.A. 1971. An overview of methods of iceberg tracking. Department of National Defence. Proceedings of the Canadian Seminar on Icebergs, Halifax, Nova Scotia.

Kerr, D.E., editor. 1951. Propagation of short radio waves. Massachusetts Institute of Technology, Radiation Laboratory Series, 13, McGraw-Hill, New York.

Lenczyk, R.E. 1965. Report of the international ice patrol service in the North Atlantic Ocean (Season of 1964). Coast Guard Bulletin No. 50, 109 p.

Lowry, R.T., A. Stuart, J.B. Mercer and J.R. Benoit. 1984. Modelling the radar detection of icebergs. Presented at the Ninth Canadian Symposium on Remote Sensing, St. John's, Newfoundland, August 12-13, 1984.

Nathanson, F.E. 1969. Radar design principles. McGraw-Hill, New York.

Parsons, A. Tracking of meteorological buoys with X-band radar transponders. Bedford Institute of Oceanography (Communication).

Robe, R.Q. and T.S. Ellis. Tagging of arctic icebergs. Report of the International Ice Patrol in the North Atlantic Ocean (Season of 1977), Coast Guard Bulletin No. 63.

Robe, R.Q. and T.S. Ellis. 1978. Tagging of arctic icebergs, Arctic Bulletin, 2(14).

Ryan, J.P., M.J. Harvey and A. Kent. 1985a. Assessment of marine radar for the detection of icebergs. Environmental Studies Revolving Fund Study 655008.

Ryan, J.P., M.J. Harvey. 1985b. Assessment of marine radar for the detection of ice and icebergs (Program Extension). Environmental Studies Revolving Fund Study, Report in Preparation.

Sittrop, M. 1977. On the sea - clutter dependency on wind speed. Radar-77, International Conference, London, England, October 25-28, 1977.

Skolnik, M.I. 1970. Radar handbook. McGraw-Hill, New York.

Walsh, J., S. Srivastava, and B. Dawe. 1985. Remote sensing of icebergs by HF ground wave doppler radar. Proceedings 1985 North American Radio Science Meeting, Vancouver.